LUND UNIVERSITY
Faculty of Science

A mean-field approach to attractive few-body Fermi gas

Morten Piibeleht

Thesis submitted for the degree of Master of Science
60 ECTS

Supervised by S.M.Reimann, G.Carlsson

Department of Physics
Division of Mathematical Physics
May 2016

Abstract

Quantum many-body systems can be studied theoretically from first principles using microscopic models, but the computational cost of numerically exact calculations increases exponentially with the number of particles and the complexity of the interaction, limiting the systems that can be analysed. The Hartree-Fock-Bogoliubov (HFB) and quasiparticle random phase approximation (QRPA) methods, heavily used in nuclear physics, rely on mean-field approximations but scale more favourably with increasing system size and complexity. In this work we apply these methods to the problem of a two-dimensional harmonically trapped Fermi gas with attractive interactions, with the goal of investigating the validity of the approximations in the few-body limit.

We implement the approximate methods in code and then compare them with exact calculations. We find that the HFB method can account for pairing correlations that arise due to the attractive interaction, predicting well the ground state energy even at high interaction strengths. Also, the excitation spectra predicted by the QRPA method qualitatively match the true spectra, reproducing the expected subset of excitations. Finally, we see that perturbative corrections can be used to improve the ground state energy estimate of the HFB.

Popular summary

The past hundred or so years have shown us that if the microscopic world is to be described, quantum mechanics has to be invoked. It allows us to make accurate predictions on the scale of atoms and smaller, and at very low temperatures, down all the way to absolute zero. Whether it is a few tens of electrons whirling around in the electron cloud of an atom, or the billions of them navigating the crystal structure of piece of metal, we have the basic description down.

However, the difficulty with exact, first principles approaches is that the calculations can be computationally expensive. You could generally say that the cost originates from two sources: the size of the system, like the number of particles, and the complexity of the system – the finer the details the system exhibits, the higher the accuracy needed for the calculations.

As an example, with several interacting particles, we have to account for the interaction between every pair. With more and more particles, the number of interacting pairs we have to keep track of will grow faster than the number of particles itself, and therefore the calculations can only be performed for relatively small systems. And by small we mean really small – going past a dozen particles is generally a major achievement.

But then, how do we study these systems? The answer is "approximations". What it means is that by using reasonable assumptions we reformulate and simplify the original problem, making the calculations easier. For example, instead of tracking every interaction between each pair of particles, we could instead approximate the interaction as an average effect from all the particles. That is, we say that every particle feels an average force from all the other particles, instead of being aware of them individually.[1]

However, with approximation methods it can be difficult to know how well they work. In general, you could say that approximations always have a region of validity and outside of that region the method does not yield good results. Averaging the interaction would fail

[1]This is in a nutshell the Hartree-Fock method, which is widely used in quantum physics.

to describe the case where particles prefer to form pairs.

This work looks at a method that is basically averages out the interaction, but in a slightly more advanced way. It should also be able to account for the pairing between the particles, but the question we are asking is how well does it actually work. Our strategy? To compare the exact and approximate methods in the limit where it is possible to solve both. We will then find out how well it works and try to understand the source of any differences.

It turns out that the method can actually reproduce the relevant features reasonably well when we compare against the exact results. Some care is necessary when interpreting the results, but it seems that we have a tool at our disposal that we can use to probe larger systems than was possible before.

Contents

List of acronyms

HF	Hartee-Fock
HFB	Hartree-Fock-Bogoliubov
QRPA	Quasiparticle Random Phase Approximation
pp	particle-particle
ph	particle-hole
hh	hole-hole

Chapter 1

Introduction

The quantum many-body problem is at the core of many branches of modern physics, applicable to a plethora of systems, such as the electron clouds of an atom, atomic nuclei, solid state systems, cold atomic gases and so forth. Setting up the mathematical description for these problems can be quite straightforward, but actually solving them is difficult and a source of many open research questions.

Broadly speaking, we could say that there are two edge cases that are most often studied. For very small systems it is feasible to solve the full many body problem exactly (usually numerically). But if the system is larger than a dozen or so particles, or exhibits complex behaviour, then the computational cost of this approach becomes too great. On the other hand, approximate methods, such as mean field methods, allow us to investigate the large particle number limit. The problem with them is that the results can be hard to trust, since it is difficult to know the quality of the approximation.

In this work we are interested in bridging the gap between the two extremes. We apply mean-field methods to the few-particle case and see how well they perform. This allows us to evaluate if the mean-field methods are a good way of studying the emergence of the many-body limit from microscopic principles.

We constrain ourselves to attractively interacting Fermi gases. This is because many-body systems can also be studied with experimental methods and cold atom gases especially allow for precise and highly tunable experiments, that can be used to verify or refute theoretical models [7, 8].

In such systems, as one changes the interaction strength, mean-field models predict a quantum phase transition from a normal phase to a superfluid phase. This phase transition should be visible in the excitation spectra as well, with the angular-momentum conserving

excitation showing up as a Higgs mode in the superfluid phase [9]. Recently the few body case was calculated and preliminary results hint at the emergence of the Higgs mode with increasing particle number [5].

In this work we lay the groundwork for extending those few body calculations using mean field methods by investigating how well the Hartree-Fock-Bogoliubov (HFB) method works in the few body limit for this particular physical system. We access the excitation spectra by building a random phase approximation calculation (QRPA) on top of the HFB solution.[1] We then compare the results from the HFB and QRPA calculations directly against the exact solutions, which allows us to immediately evaluate the method's quality.

Thesis outline.

- Chapter 2 gives an overview of of the background and basic assumptions that underlie this work, and we also define the physical system we study. We also briefly discuss the mean-field solution, the Higgs mode and its few-body precursor, which is the driving motivator of this work.

- Chapter 3 explores the Hartree-Fock-Bogoliubov method, by giving an overview of the method, explaining how the method was implemented in code and then used for estimating the ground state energy of the many-body system.

- Chapter 4 looks at the QRPA method, by explaining its implementation, calculating and compare the excitation spectra, and makes a first attempt at calculating the lowest monopole excitation using this approximate method. We also take a look at a way to calculate a correction to the HFB ground state energy estimate.

Author's contributions. In this work the author wrote a set of modules in the Julia language [2, 4], that implement the Hartree-Fock, HFB and QRPA methods, so that calculations in a truncated two-dimensional harmonic oscillator basis can be performed. Aspects of the implementation are discussed in chapters 3.2, 4.2 and appendix A.

The author then used the code to calculate the expectation values with both the new library and a pre-existing exact diagonalization library in order to compare the results. The results of the comparison are presented in subchapters 3.3, 4.3, 4.4 and 4.5.

[1] Both the HFB and QRPA methods are discussed in various nuclear physics textbooks, such as [18].

Chapter 2

Many-body quantum systems

While quantum theories consistent with special relativity can be formulated, and are for example the basis for elementary particles physics in the form of the Standard Model, non-relativistic models are often sufficient to accurately describe many of the physical systems of interest. They can be used to describe low temperature gases and liquids, solid state systems, electrons in atoms, atomic nuclei and so forth. However, these systems generally have many interacting particles, making theoretical studies difficult. This primarily due to how fast the computational complexity grows with the increasing system size and complexity. Numerically exact solutions are usually only possible for very few particles and beyond that we have to resort to additional approximations.

Experimental investigation of these systems can also be difficult, since the systems are generally hard to control and measure. An exception to that are the cold atom gases, that can supply us with table-top versions of quantum systems where we can tune parameters and perform accurate measurements. They still exhibit quantum phenomena and so we can generalize some of the insights gained by studying quantum gases to other systems.

In this chapter we briefly look at cold atom gases and how they are useful for the study of quantum systems. We then introduce the second quantization formalism and make some remarks regarding numerical calculations. Finally, as a specific system of interest, we study a harmonic trap with attractively interacting fermions.

2.1 Cold atom gases

Ultracold atomic gases are physical systems of particular interest to us. They are governed by the same laws as other microscopic quantum systems, but they are more easily experi-

mentally controlled. Therefore they can be used to experimentally realize various quantum systems in order to investigate quantum effects. This means that they can effectively function as simulations of other quantum systems [7].

Over the past decades the field has made significant progress, with various experimental and theoretical techniques available for the study of these systems [8]. This has given insights into the behaviour of quantum systems in various regimes, such as the formation of long-distance pairs for weakly interacting systems or the condensation of bosonic pairs in the strongly interacting limit.

Depending on the choice of the atom, the constituent particles can be either bosons or fermions. The particles are then usually trapped using a mageneto-optical trap, which yields an approximate harmonic potential that confines the particles. Laser light is also used to cool down the gas to the microkelvin levels. Finally, magnetic fields via Feshbach resonances [12] can be used to tune the interaction.

Much of that work deals with the many body limit and strongly correlated system, and then the theoretical approaches often rely on mean field models. This immediately creates an interesting question – how does the mean field behaviour emerge from the microscopic? Similarly, at what system size does the mean field description become accurate?

In recent years it has become possible to experimentally prepare few particle fermion systems [24]. Pairing effects and the transition from few to many body has also been studied experimentally using this technique [26, 27]. This has also opened up the possibility of studying other phenomena, such as quantum magnetism or quantum information processing, in this few-body regime.

2.2 The many-body formalism

The single particle quantum mechanics can systematically be extended into the second quantization formalism which can describe many-body systems. Numerous books cover this topic in great detail [23, 16, 6] and others more offer brief summaries [18], so here we only make a short introduction to the parts relevant to this work.

It is possible to identify two fundamental principles that underlie the quantum many-body model. That is, the many body theory (a) builds on top of a known single-particle model, and (b) is still a quantum theory.

Mathematically a quantum theory is described by a Hilbert space. (a) just means that we have a Hilbert space $\mathscr{H}_1$ of single-particle quantum states. The second principle implies

that a A-particle system is also described by a Hilbert space, $\mathscr{H}_A$. Finally, these two spaces have to be related, namely there should be a way of constructing a minimal many body Hilbert space using just the single-particle space. Mathematically this is captured by the notion of a tensor product of vector spaces [1], so that the A-particle space is built from the single particles spaces as follows

$$\mathscr{H}_A = \underbrace{\mathscr{H}_1 \otimes \ldots \otimes \mathscr{H}_1}_{A \text{ times}}$$

We additionally have the 0-particle space $\mathscr{H}_0$ as well, which represents the vacuum case, and it would only contain the state $|0\rangle$, representing the case of no particles. Now that we have all these vector spaces, we can go one step further and add them all together using a direct product to form a single Hilbert space that can represent all physical states.

$$\mathscr{H} = \mathscr{H}_0 \oplus \mathscr{H}_1 \oplus \mathscr{H}_2 \oplus \ldots$$

There is one more complication that we have to deal with – it is the idea that elementary particles are fundamentally indistinguishable. Our description so far assumes that we can identify a "first" particle, a "second" particle and so forth. This means that only a subset of many particle states represent physical states, namely the ones that are either symmetric or antisymmetric under particle exchange, corresponding to bosons and fermions respectively.

In order not to go into too much detail on this matter we can just introduce the creation and annihilation operators $c_k^\dagger$ and c_k. There is one of each for every single particle state k and intuitively they are defined as operators that when they act on a state, the creation operator adds a particle in the state k to the state, and the annihilation operator removes it. We also assume that it creates particles in the symmetric or antisymmetric manner, keeping the states consistent.

Many-body states that contain specific particles can then be built from the vacuum, by acting on it with the creation operators. That is, single particle states can be created as $|i\rangle = c_i^\dagger |0\rangle$, and higher particle-number states with consecutive applications of creation operators.

For fermions, which are the particles of interest in this work, the creation and annihilation operators satisfy anticommutation relations

$$\{c_i, c_j\} = 0 = \{c_i^\dagger, c_j^\dagger\}, \quad \{c_i, c_j^\dagger\} = \delta_{ij}$$

[1] A clear definition the tensor product can be found in [19].

These are equivalent to saying that the states have to be antisymmetric and also imply that there can only be one particle in each orthogonal single particle state. The last condition is consistent with the Pauli principle for fermions.

Operators in second quantization. Using the creation and annihilation operators we have a way of treating the many body state space. We now need a way of treating operators in the same formalism.

Usually in, for example, the Hamiltonian, if we need several particles, we would just add the necessary terms for every particle. For example, the kinetic term in a A-particle Hamiltonian might look like

$$\sum_{i=1}^{A} \frac{\hat{\mathbf{p}}_i^2}{2m}$$

This is insufficient for a many-body formalism, since the number of particles should not be defined on the formalism level. It does not make sense to say that "an operator acts on the i-th particle", or "on the i-th and the j-th". Also, we should have the same Hamiltonian describing the system, independent of how many particles there are in the system.

Instead, in the many-body formalism we have the concept of operators being a one-body operators, two-body operators, and so on. One body operators can then be fully described by the way they act on a single particle, i.e. by a matrix with elements $\langle i|\hat{T}|j\rangle$. Similarly, a two body operator would be defined by its effect on the two-particle states, i.e. by the elements $\langle ij|\hat{V}|kl\rangle$.[2]

Once we have the matrices, the operators can be represented in the many-body formalism using just the creation and annihilation operators, and the components of these matrices. The one-body operators have then the general form

$$\hat{T} = \sum_{ij} c_i^\dagger \langle i|\hat{T}|j\rangle \, c_j$$

and the two-body operators have the form

$$\hat{V} = \frac{1}{2} \sum_{ijkl} c_i^\dagger c_j^\dagger \langle ij|\hat{V}|kl\rangle \, c_l c_k$$

Physically one-body operators describe things related to each particle (kinetic energy, ex-

[2]A small note on the notation: the states denoted by $|ij\rangle$ are not (anti)symmetrised, but instead directly constructed from the single particle basis ($|ij\rangle = |i\rangle \otimes |j\rangle \neq c_j^\dagger c_i^\dagger |0\rangle$). So, they are not physical boson or fermions states, but we can still formally perform calculations with them.

ternal potential) and two-body operators capture pairwise interactions.

A general Hamiltonian for a many body system would then look like

$$\hat{H} = \sum_{ij} c_i^\dagger \langle i|\hat{T}|j\rangle \, c_j + \frac{1}{2} \sum_{ijkl} c_i^\dagger c_j^\dagger \langle ij|\hat{V}|kl\rangle \, c_l c_k$$

This is the most general form as long as one sticks to a single type of particles and a pairwise interaction.

A special one-body operator that is useful to keep in mind is the particle number operator $\hat{N}$ that measures the number of particles and can be written in terms of the creation and annihilation operators as

$$\hat{N} = \sum_i c_i^\dagger c_i$$

and where, in principle, every term would measure the number of particles in a particular state.

2.2.1 Numerical calculations

In this work we wish to solve the many-body problem numerically. It is therefore a good place to make a few general statements regarding the practicalities associated with numerical calculations.

The states and operators have to be somehow represented in the computer. We do so by choosing an orthogonal basis and then storing the expansion coefficients. A practical issue here is that already the single particle basis is, in principle, infinite. We solve that by choosing a finite basis instead, restricting ourselves to a *model space*. The philosophy here is the same as with a Taylor or Fourier series, that for most purposes, only having the first N terms is enough to capture the function with sufficient accuracy. Similarly, for quantum mechanics problems it is often the case that as the energy increases, the components become less and less significant in the ground state, allowing us to impose an energy cut-off.

It is not obvious, however, at which point the higher order terms become insignificant enough that they can be ignored. A common method to deal with this is to solve the system at several cut-offs and see if the solution converges to a constant as one increases the cut-off.

Any numeric code that solves the many-body problem can then be written in a generic

manner, without referring to any specific basis. We only have to define the size of the basis M (indexing basis elements probably as $i = 0, 1, \ldots, M-1$) and then pass two routines to the code, $T(i,j)$ and $V(i,j,k,l)$, that are able to calculate or retrieve the respective matrix elements. In other words, the exact method of how these elements are calculated is irrelevant to the implementation of the method.

2.2.2 Exact diagonalization

In this work we compare certain approximate methods against the results from exact diagonalization[3] calculations, computed using a library developed as part of [13]. The name refers to the fact that within the model space, the method solves the many-body system exactly (within numerical errors).

The method works by considering the entire many-body basis for a fixed number of particles A. All possible, unique A-particle states that can be constructed using the creation operators form the orthonormal basis set

$$\{|a\rangle = c^\dagger_{a_1} \cdots c^\dagger_{a_A} |0\rangle\}$$

The basis is large, but finite, since the single particle basis is finite. The components of the Hamiltonian matrix can then be calculated in this basis and diagonalized using standard numerical linear algebra methods.

The primary issue with the method is that the basis size grows exponentially with both the number of shells and the number of particles. Specifically, for A fermions in an M-orbital basis, the full many-body basis has

$$\binom{M}{A} = \frac{M!}{A! \cdot (M-A)!}$$

elements. The number can be brought down by imposing additional cuts, in energy or by noting that, due to symmetries, the Hamiltonian is block-diagonal and a smaller subsystems can be solved separately. However, in the end, that only allows for a few additional particles or so, and so the method still does not scale with system size.

However, as long as convergence can be shown and numeric errors do not significantly affect the results, the method allows for microscopic calculations, that are, in principle,

[3]The *exact diagonalization* method is also referred to as *configuration interaction (CI)* [14] or *shell model calculations* [17], depending on the field.

complete, accounting exactly for all correlation effects.

2.3 2D-trapped Fermi gas

The physical system studied in this work is a Fermi gas with attractive interactions trapped in an isotropic harmonic potential. By letting the $\omega_x = \omega_y \ll \omega_z$, the system becomes quasi-two-dimensional[4], since motion in the third dimension costs too much energy to be significant for the low-lying states.

The interaction between the particles is assumed to be short-range, which means that it can be modelled with a delta-function, as long as one is able to properly renormalize it [20]. It qualitatively captures the nature of the interaction, but also agrees with experiments [26].

As such, the Hamiltonian for this system, for A-particles can then be written in the wave-function picture as

$$H = \sum_{i=1}^{A} \left(\frac{\mathbf{p}_i^2}{2m} + \frac{m\omega^2}{2}\mathbf{r}_i^2 \right) - g \sum_{i<j}^{A} \delta(\mathbf{r}_i - \mathbf{r}_j)$$

where $\mathbf{r} = (r_x, r_y)$ and $\mathbf{p} = (p_x, p_y)$ are understood to be points in a two-dimensional space. Since we are interested in the general behaviour of the system we choose all units and constant so that m, $\hbar$ and ω are all unity. With this choice, the only tunable parameter we have in the system is the strength of the interaction g.

Naturally, a convenient basis for this system is the two-dimensional harmonic oscillator basis. Every harmonic oscillator orbital then corresponds to two physical orbitals, due to the two possible spin states of the fermions. The orbitals can then be labelled by (n_x, n_y, s). More details about the practical calculations in the harmonic oscillator basis can be found in appendix A.

The orbitals can be divided up into shells, by grouping the orbitals with degenerate energy together (or equivalently, orbitals with the same $n = n_x + n_y$). Figure 2.1 illustrates the 2D harmonic oscillator basis, where we see the shell structure of the oscillator and how the degeneracy of the shells increases with increasing energy.

The number of shells included in the model is a convenient way of defining a cut on the single particle basis. That is, if we say that we have N shells, then it means that we only

[4]As a practical side note, in experiments a ten-fold difference in the trapping frequencies is enough to make the system behave in a quasi-2D manner [24].

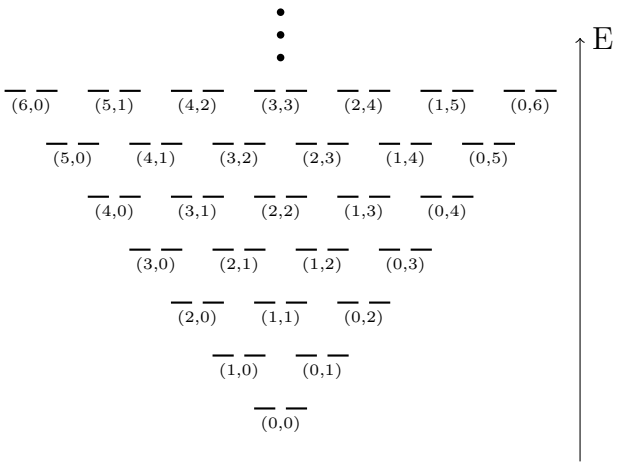

Figure 2.1: Illustration of the two-dimensional harmonic oscillator single-particle basis. Every dash represents a basis state and the states are grouped into (n_x, n_y) subshells with two spin states in every subshell. The states then further form a shells with degenerate energy $E \sim n_x + n_y$.

include the orbitals for which $n_x + n_y < N$ holds. The number of orbitals included then is $M = N(N + 1)$.

We can now illustrate the exponentially increasing computational complexity of the exact diagonalization method. A back of the envelope calculation shows that if the Hamiltonian is to be represented as a dense matrix of 64-bit floats, the memory required in the case of 30 000-element basis would be about 7 GiB, and for 70 000-element basis about 37 GiB, giving us an idea how big a basis can be before the calculations become infeasible. In table 2.1 we see the size of the basis for various numbers of particles and shell cuts. We see that only very small systems indeed (up to few particles and shells) are feasible.

By using symmetries of the Hamiltonian, the many-body basis can be reduced down to elements with zero spin and angular momentum, without affecting the exactness of the calculations. This significantly reduces the size of the basis, but the general exponential dependence remains, and we therefore only gain a few additional shells or particles. This in turn limits the available model spaces in which we can perform comparisons with the exact solutions.

Once we have constrained ourselves to a particular model space, exact diagonalization yields exact solutions. We can then apply further approximations (such as mean-field) within this model space, and compare the results against the exact solution. Working within a particular model space, we gain insight into how well the approximations works.

We should note a few potential drawbacks here. First, to get physically relevant results

Table 2.1: Size of the complete basis for exact diagonalization as a function of the number of shells and particles. The cases in bold require more than 8 GiB of memory to store as a dense matrix of 64-bit floats.

		Number of shells (N)						
		2	3	4	5	6	7	8
Number of particles (A)	1	6	12	20	30	42	56	72
	2	15	66	190	435	861	1540	2556
	3	20	220	1140	4060	11 480	27 720	**59 640**
	4	15	495	4845	27 405	**111 930**	**367 290**	$\mathbf{1.0 \times 10^6}$
	5	6	792	15 504	**142 506**	**850 668**	$\mathbf{3.8 \times 10^6}$	$\mathbf{1.4 \times 10^7}$
	6	1	924	**38 760**	**593 775**	$\mathbf{5.2 \times 10^6}$	$\mathbf{3.2 \times 10^7}$	$\mathbf{1.6 \times 10^8}$
	7	-	792	**77 520**	$\mathbf{2.0 \times 10^6}$	$\mathbf{2.7 \times 10^7}$	$\mathbf{2.3 \times 10^8}$	$\mathbf{1.5 \times 10^9}$
	8	-	495	**125 970**	$\mathbf{5.9 \times 10^6}$	$\mathbf{1.2 \times 10^8}$	$\mathbf{1.4 \times 10^9}$	$\mathbf{1.2 \times 10^{10}}$
	9	-	220	**167 960**	$\mathbf{1.4 \times 10^7}$	$\mathbf{4.5 \times 10^8}$	$\mathbf{7.6 \times 10^9}$	$\mathbf{8.5 \times 10^{10}}$
	10	-	66	**184 756**	$\mathbf{3.0 \times 10^7}$	$\mathbf{1.5 \times 10^9}$	$\mathbf{3.6 \times 10^{10}}$	$\mathbf{5.4 \times 10^{11}}$
	11	-	12	**167 960**	$\mathbf{5.5 \times 10^7}$	$\mathbf{4.3 \times 10^9}$	$\mathbf{1.5 \times 10^{11}}$	$\mathbf{3.0 \times 10^{12}}$
	12	–	1	**125 970**	$\mathbf{8.6 \times 10^7}$	$\mathbf{1.1 \times 10^{10}}$	$\mathbf{5.6 \times 10^{11}}$	$\mathbf{1.5 \times 10^{13}}$

we should systematically increase the size of the model space and check for convergence. That would also be the only way to see if the method gets better or worse with increasing model space and system size. Furthermore, restricting ourselves to a particular model space may introduce artificial, non-physical features, which we should be mindful about. However, as a first step this is sufficient and it is generally possible to see the behaviour for the first few steps and make some preliminary extrapolations based on that.

Having fixed a model space, we can now solve the system and see how it generally behaves with changing interaction strength. In figure 2.2 we see the ground state energy as a function of the interaction strength of a two-particle system for various numbers of shells. Very generally, we see that as the interaction strength goes up, the energy of the ground state gets pulled further and further down.

An effect to keep mind here is that the energies do not converge with increasing number of shells, which is due to the pathological behaviour of the delta-function interaction in two or more dimensions [20]. In a nutshell, the issue is that the off-diagonal elements of the interaction matrix do not fall off fast enough. For physics calculations a renormalization scheme is necessary and can be achieved by considering the binding energy in a two-body system. For us it implies that in order to have comparable results, we perform both the exact and approximate calculations in exactly the same model space.

Finally, in figure 2.3 we see the excitation spectra for two cases – an open and a closed

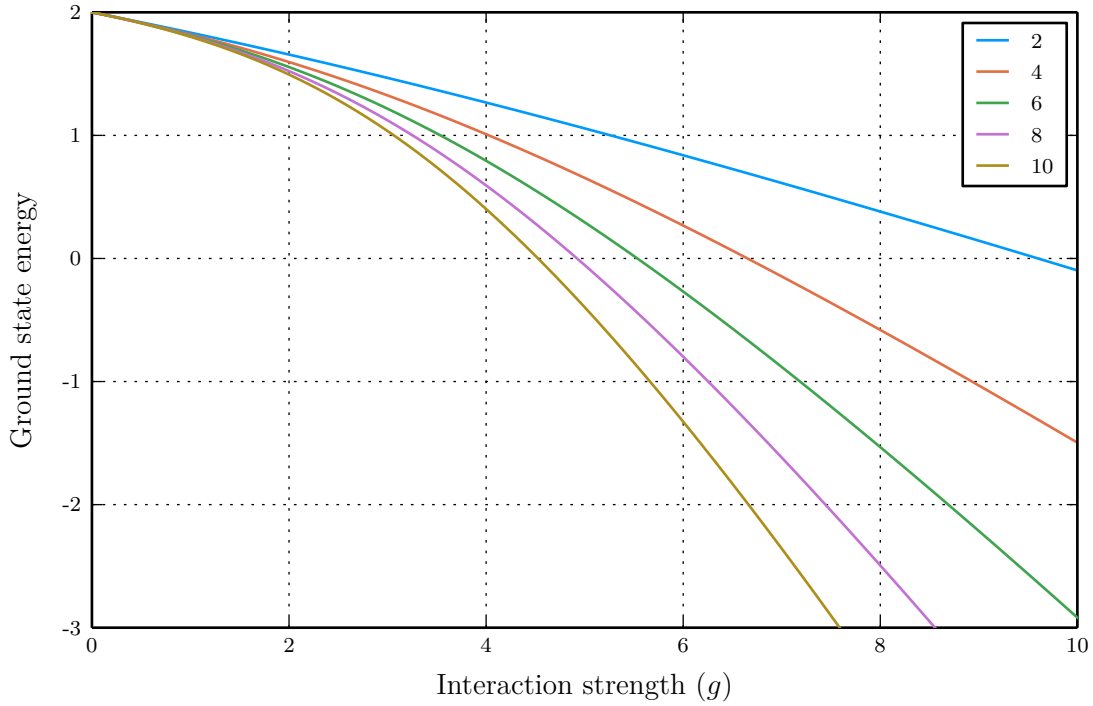

Figure 2.2: The ground state energy of a two-particle system for various number of harmonic oscillator shells, calculated with exact diagonalization.

shell. A closed shell means that there is just enough particles to fill the lowest shells completely (in the non-interacting limit). In the open shell case the highest shell is not completely filled, which also leads to a degeneracy in the ground state in the non-interacting limit. Due to these differences, these two cases will behave differently, which we will see later on.

2.3.1 Higgs mode

The system has been studied in the large particle number limit using field-theoretic and methods and mean-field approximations [9]. For a closed shell case these calculations predict a quantum phase transition as one increases the interaction strength, with the system suddenly moving from a *normal phase* to *superfluid phase* after a critical interaction strength value. More precisely, the solution for the ground state before the phase transition does not exhibit any pairing correlation, but does so in the superfluid phase after the phase transition.

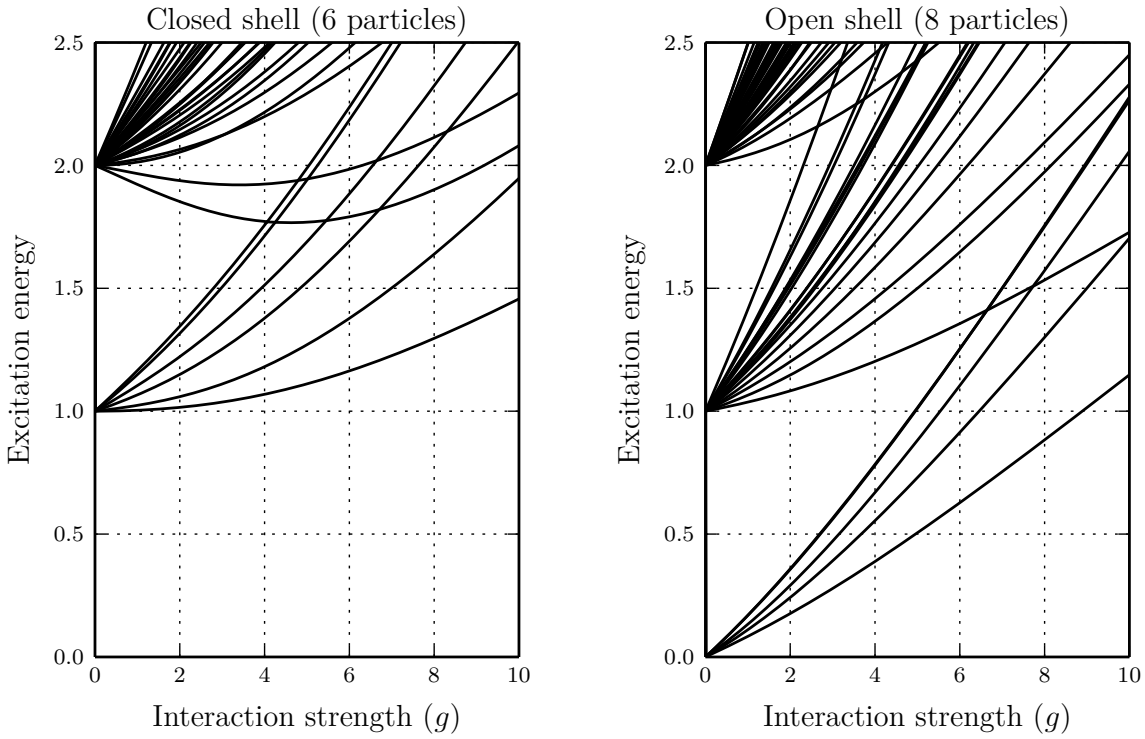

Figure 2.3: An example excitation spectra of the closed and open shell systems, as calculated with exact diagonalization with three oscillator shells.

The phase transition point is shown very clearly in the energy of the lowest monopole excitation[5], visible in figure 2.4. We see there that the many-body calculations (the black lines) predict that at the phase transition point the excitation does not cost any energy and the ground state is degenerate.

These results can be interpreted in terms of the shape of the free energy surface as it changes with the changing interaction strength. Schematic shapes of the free energy surfaces are shown in figure 2.5. If the we note that the ground state of the system corresponds to the minimum of the free energy, then we see that for weak interactions, in the normal phase, the ground state is expected to be $\Delta = 0$, implying no pairing in the state. However, after the phase transition, the minimum shifts to a non-zero pairing field, which means that the ground state now exhibits pairing.

The lowest monopole excitation can be interpreted as being an oscillation on the free energy surface in the pairing field Δ. The excitation energy is then related to curvature of

[5]A *monopole excitations* is an excitation with zero angular momentum.

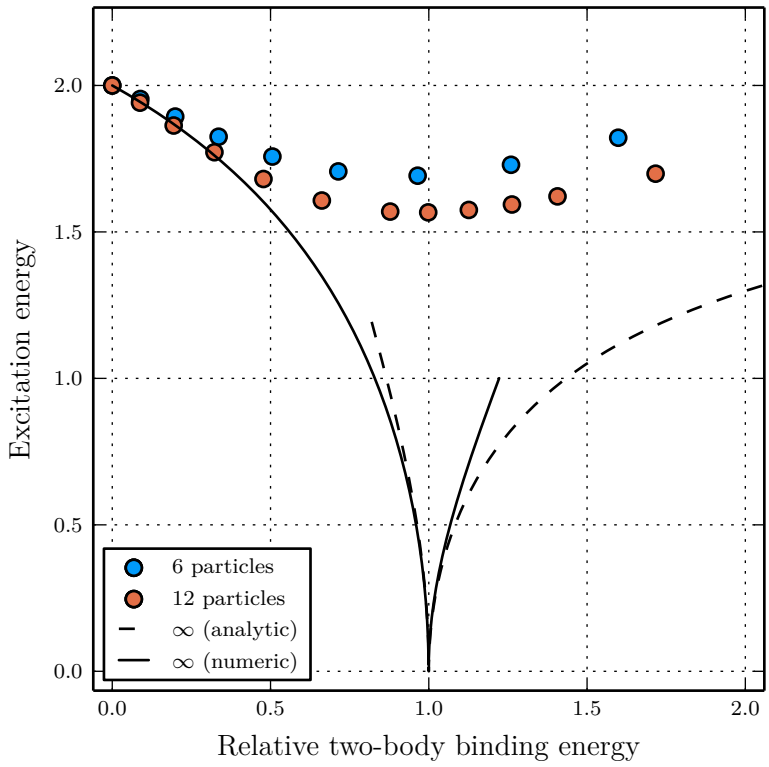

Figure 2.4: Excitation energies of the lowest monopole excitation. The solid (dashed) line corresponds to the numeric (analytic) solution of the many-body case, and the points are few-body body calculation performed using exact diagonalization for 6 and 12 particles. The two-body binding energy on the x-axis is effectively equivalent to the interaction strength g. Adapted from [5].

the free energy surface near the minimum. It is then clear that before and after the phase transitions we expect a non-zero excitation energy, whereas at the phase transition, where the free energy surface becomes flat, the excitation energy should becomes zero. This interpretation of the excitation in terms of the "Mexican hat" potential in the superfluid phase is why it is often referred to as the Higgs mode.

In figure 2.4 we also see results from exact few-body calculations, originally presented in [5]. The few-body calculations show us that while there is no sharp phase transition, the lowest monopole excitation does have a characteristic minimum. Furthermore, as the number of particles increases we see that the minimum deepens, implying that it is a precursor to the Higgs mode, yielding a sharp transition if we allow the number of particles to be large enough.

Due to the high computational cost of exact calculations, only six and twelve particle cases were calculated, with the next closed shell case not being feasible any more. This is

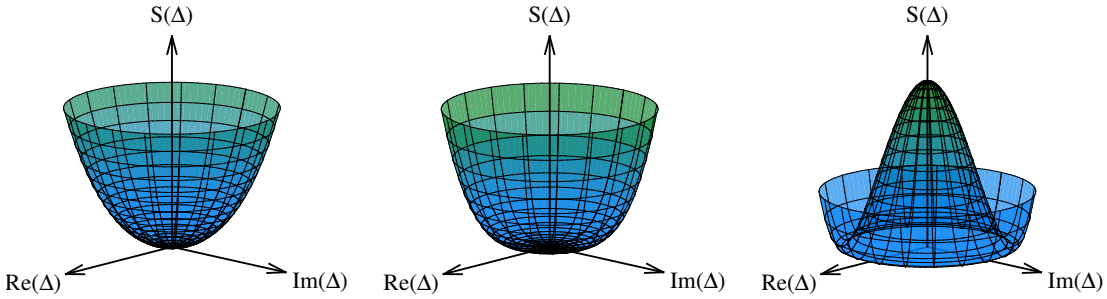

(a) normal phase (b) critical point (c) superfluid phase

Figure 2.5: Sketches of the system's free energy surfaces as a function the pairing field Δ in different regimes (determined by the interaction strength). Excitations of the system can be interpreted as being oscillations in this potential field. A more rigorous discussion can be found in [9].

the primary motivation of this work: to find other methods that would be able to reach larger system while still producing results consistent with the few-body calculations.

Finally, we just briefly note that for open shell cases the mean field approach predicts that the ground state will have pairing for all values of the interaction strength, meaning no phase transition nor degeneracy in the mean-field predictions. The few-body results are also consistent, with the excitation energy increasing monotonically with the interaction strength in the open shell case.

Chapter 3

Hartree-Fock-Bogoliubov method

As we discussed in the previous chapter, a full, first principles, exact solution to the quantum many-body problem is computationally difficult due to the exponentially increasing size of the matrices as one increases the number of particles and the size of the single-particle basis. It is therefore necessary to use approximate methods if we desire to extend our calculations to these systems.

In this chapter we examine the Hartree-Fock-Bogoliubov (HFB) method, one such option. It is widely used in nuclear physics to study the ground state of a nucleus and is thoroughly discussed in various books [18, 6] and articles [3]. It generalizes the Hartree-Fock[1] and BCS[2] methods, allowing us to optimize the single particle basis and describe pairing between particles at the same time. For an attractive interaction one intuitively expects that particles would pair up more and more with increasing interaction strength, and that therefore such correlations would be significant.

Specifically, we are interested in the method's applicability to the two-dimensional Fermi gas, described in the previous chapter. For this we implement the HFB method in code, solve the system in the few-body limit and then compare the results with exact calculations.

[1] A mean field method that approximates the wave function using a single Slater determinant, but optimizes the single particle basis. It is, due to the nature of the approximation, completely unable to account for correlations (with the exception of Pauli correlations).

[2] A method with a different guess for the wave function, accounting for some amount of correlations, but not optimizing the single particle basis itself.

3.1 Formulation

The starting point of the HFB method is the Bogoliubov transformation, which is a unitary transformation among the creation and annihilation operators. It defines a new set of operators β_k, that are called quasiparticle operators, with the name stemming from the interpretation that the operators acting on an appropriately defined vacuum state can create and annihilate quasiparticles. The transform, however, can mix creation and annihilation operators together, so the quasiparticles do not have a clear interpretation of being physical particles.

If the single particle basis has M elements, then the transformation is defined by two complex $M \times M$ matrices U and V, so that

$$\beta_k^\dagger = \sum_i U_{ik} c_k^\dagger + V_{ik} c_i$$

We can formally organize the transformation into a $2M \times 2M$ matrix

$$\mathcal{W} = \begin{pmatrix} U & V^* \\ V & U^* \end{pmatrix}, \quad \text{so that} \quad \begin{pmatrix} \beta \\ \beta^\dagger \end{pmatrix} = \mathcal{W}^\dagger \begin{pmatrix} c \\ c^\dagger \end{pmatrix} = \begin{pmatrix} U^\dagger & V^\dagger \\ V^T & U^T \end{pmatrix} \begin{pmatrix} c \\ c^\dagger \end{pmatrix}$$

and by requiring the matrix $\mathcal{W}$ to be unitary, we ensure that the quasiparticle operators satisfy the canonical commutation relations.

The quasiparticle vacuum is the state $|\text{HFB}\rangle$, defined as the vacuum of the quasiparticle annihilation operators[3], i.e.

$$\forall k : \beta_k \, |\text{HFB}\rangle = 0$$

Such a state always exists and is non-trivial and unique. The converse is not true – multiple Bogoliubov transformations can define the same state (e.g. phase freedom).

A useful feature of the HFB state is that it is uniquely defined by the normal and abnormal density matrices ρ and κ, which are defined by

$$\rho_{ij} = \langle \text{HFB} | c_j^\dagger c_i | \text{HFB} \rangle = (V^* V^T)_{ij}, \quad \kappa_{ij} = \langle \text{HFB} | c_j c_i | \text{HFB} \rangle = (V^* U^T)_{ij}$$

The densities can also be joined into a $2M \times 2M$ matrix, called the generalized density

[3]This definition is helpful when calculating expectation values of the HFB state. If an operator is expressed in terms of the c_k and $c_k^\dagger$ operators, then it can also easily be expressed in terms of quasiparticle operators. Certain terms can then be discarded immediately and others evaluated easily.

matrix

$$\mathcal{R} = \begin{pmatrix} \rho & \kappa \\ -\kappa^* & 1-\rho^* \end{pmatrix}$$

The densities can, in principle, be calculated for any many-body state, but a many-body state is a HFB state if and only if the generalized density matrix is idempotent, i.e. $\mathcal{R}^2 = \mathcal{R}$.

HFB equations. So far we have only discussed HFB states generally. In order to approximate the ground state with it, we turn to the variational principle to derive a set of equations, which, when solved, will yield the best approximation to the ground state. Mathematically this means that we minimize the energy expectation value $E = \langle \mathrm{HFB}|\hat{H}|\mathrm{HFB}\rangle$ with respect to changes in the Bogoliubov transformation (or equivalently, in the densities). We assume that $\hat{H}$ is given in terms of the creation and annihilation operators as

$$\hat{H} = \sum_{ij} T_{ij} c_i^\dagger c_j + \frac{1}{4} \sum_{ijkl} \bar{v}_{ijkl} c_i^\dagger c_j^\dagger c_l c_k$$

where in turn the matrix elements of T and $\bar{v}$ are to be calculated as

$$T_{ij} = \langle i|\hat{T}|j\rangle\,, \quad \bar{v}_{ijkl} = \langle ij|\hat{V}|kl\rangle - \langle ij|\hat{V}|lk\rangle$$

A complication arises from the fact that we can not explicitly specify the particle number of a HFB state in advance, and, in general, it does not even have a well-defined particle number. We solve this by imposing a constraint on the particle number expectation value, $\langle \mathrm{HFB}|\hat{N}|\mathrm{HFB}\rangle = A$. This introduces a Lagrange multiplier μ into the equations or, equivalently, we could say that we minimize the Hamiltonian $\hat{H}' = \hat{H} - \mu\hat{N}$ under the aforementioned constraint.[4]

After applying the variational principle we are left with the HFB equations, which can be expressed compactly in matrix form as

$$\begin{pmatrix} h & \Delta \\ -\Delta^* & -h^* \end{pmatrix} \begin{pmatrix} U_k \\ V_k \end{pmatrix} = E_k \begin{pmatrix} U_k \\ V_k \end{pmatrix}$$

[4]The Lagrange multiplier μ can also be interpreted as a chemical potential.

where[5]

$$h = T + \Gamma - \mu, \quad \Gamma_{ij} = \sum_{kl} \bar{v}_{iljk}\rho_{kl}, \quad \Delta_{ij} = \frac{1}{2}\sum_{kl} \bar{v}_{ijkl}\kappa_{kl}$$

By solving these equations we get the HFB approximation for the ground state. However, it should be noted here that the equations are non-linear, since h and Δ depend on the HFB state itself, and solving them is not entirely trivial.

Finally we note that we can identify two qualitatively different sets of HFB states. If the abnormal density κ is non-zero, then the state mixes subspaces of different particle number, but also includes some amount of correlations. If instead $\kappa = 0$, then the state can be represented by just a single Slater determinant of some single-particle creation operators[6], and therefore does not incorporate any correlations apart from Pauli correlations. It is a curious feature of the HFB method that pairing correlations are incorporated into the HFB state by mixing subspaces with different particle numbers.

If we then look at the ground state as a function of some parameter, such as the interaction strength, then we may see that a certain parameter range yields one type of solution and another a different type of solution. The point where one solution changes into another is then called a quantum phase transition and the region with non-paired solution ($\kappa = 0$) is often referred to as the *normal phase* and the region with pairing and particle number mixing as the *superfluid phase*.

3.2 Implementation

As part of this work we implemented the HFB method as a Julia [4] module in order to perform numerical calculations. The code was organized in such a way that the algorithm only needs to know the size of the single-particle basis and then accepts the routines that calculate the matrix elements of the $\hat{T}$ and $\hat{V}$ operators and the desired particle number as input.

The HFB states are represented in computer memory by the two $M \times M$ complex matrices U and V. As a practical optimization, the ρ and κ matrices are also calculated and stored. Using U and V (or ρ and κ) we can calculate various expectation values of the

[5] h, Δ, T and Γ are understood to be $M \times M$ matrices, but μ is just a real number multiplied by the identity matrix in the matrix equations.

[6] A Hartree-Fock state, for readers familiar with that method.

HFB state. The energy expectation value can be calculated by

$$\langle \hat{H} \rangle = \mathrm{Tr}\left(T\rho + \frac{1}{2}\Gamma\rho - \frac{1}{2}\Delta\kappa^* \right)$$

and the average particle number by $\langle \hat{N} \rangle = \mathrm{Tr}(\rho)$.

In order to get the ground state of the system we have to solve the HFB equation. As we mentioned before, the equation is non-linear, with Γ and Δ depending on the U and V. It is therefore necessary to employ an iterative scheme, where we start with an initial guess for the HFB state, calculate the h and Δ and then diagonalize the matrix. The eigenstates with positive eigenvalues are then used to define the U and V matrices of the next iteration. With every iteration the solution then converges towards the minimum and we can stop iterating once the change in energy between iterations is sufficiently small.

Additionally, on every iteration we have to choose an appropriate value for μ since it is not known a priori. We do it by trying out various guesses until we get a value that yields a particle number expectation value that is close to the desired value.

Specifically, we chose a very simple binary search scheme. This is possible since the particle number is a monotonically increasing function of μ, illustrated in figure 3.1. We first try $\mu = 0$ and decide whether we should move in the positive or in the negative μ direction. Then we try ± 1 and after that we start doubling μ up- or downwards until the desired particle number is somewhere between the two extremes. Finally we employ a binary search to find the value μ where the particle number is equal to the desired value within a predefined error. Special care has to be taken in the normal phase where the particle number becomes a step function of μ – there we find the minimum and maximum values separately and then choose their average as our guess for the μ.

Figure 3.2 shows the convergence of the energy expectation value for a closed shell case. The general behaviour is that the energy converges exponentially to a stationary value. In the same figure we also see that the speed of convergence is fast for both the normal and superfluid phases, but increases significantly near the phase transition.

The Hartree-Fock (HF) method. In addition to the exact solution, it is also interesting to compare the HFB against the non-correlated Hartree-Fock solution. While it could be thought of as a separate method, we can also see it as a special case of the HFB method, where we enforce $\kappa = 0$. When using the iterative scheme, it is in fact clear from the equations that if we use a HF ($\kappa = 0$) state as the initial guess, then the solution will

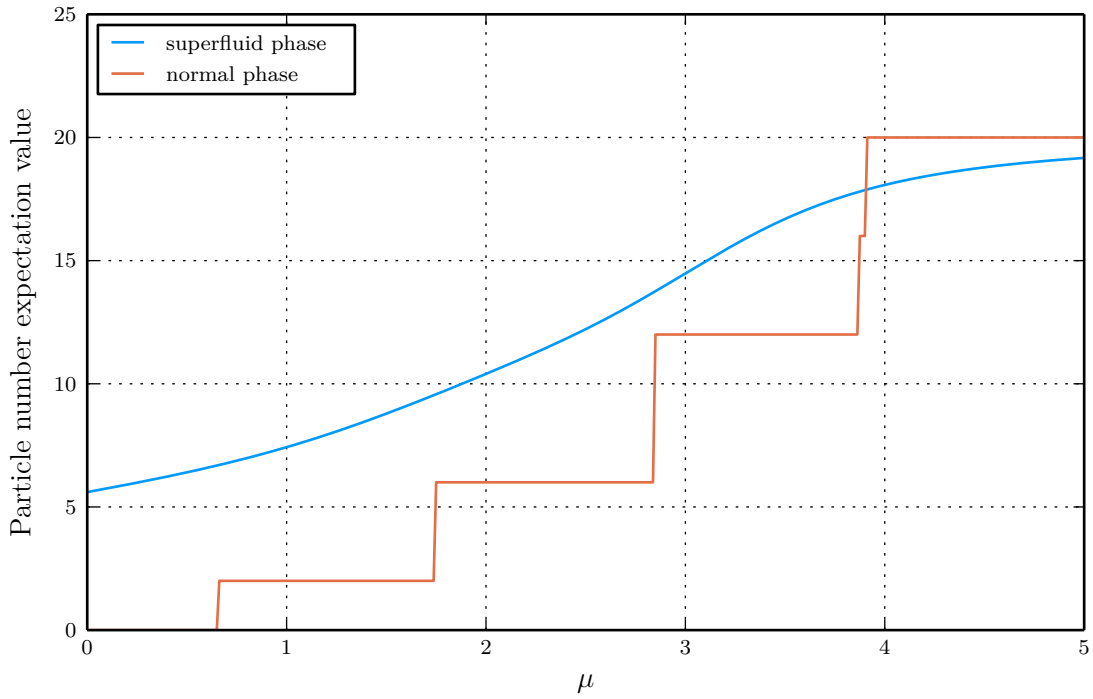

Figure 3.1: The particle number expectation value of the HFB solution when solving the HFB equation with fixed fields Γ and Δ for various μ values. The fixed fields correspond to the converged solution of a 6-particle closed shell system and we look a two different interaction strengths, corresponding to the normal and superfluid phases.

also be a HF state, making the enforcement of this requirement quite simple.

In this work we implemented a separate routine for the the Hartree-Fock calculations, but the results are consistent with this special case approach.

3.3 Ground state energy

Using the implementation described in the previous chapter, we can now estimate the ground state energies of systems with the HF and HFB methods. We now compare those estimates with exact results for the Fermi gas system described in chapter 2.3, with both the exact and approximate calculation done in the same truncated harmonic oscillator model space.

Figure 3.3 shows how the absolute value of the energy depends on the interaction strength g for the three different methods (exact, HF and HFB). Broadly speaking, we see

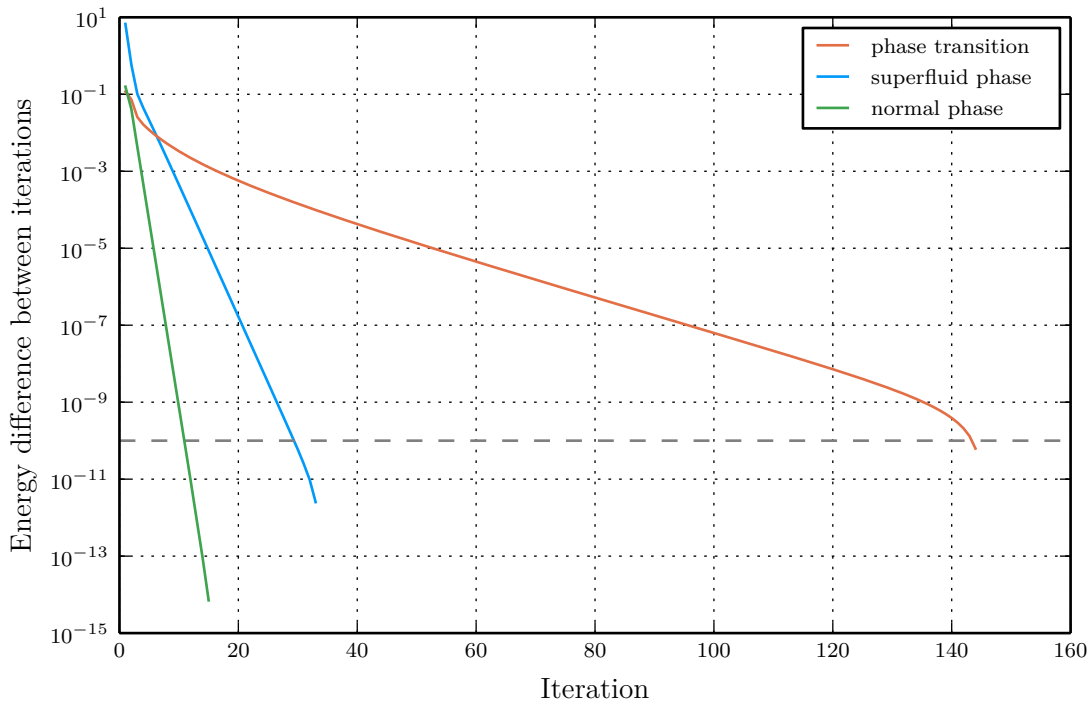

Figure 3.2: The convergence of the HFB solutions in a closed shell case (6 particles, 3 shells) for different interaction strengths.

that the methods follow the exact value of the energy, with the variational methods always giving an estimate that is higher than the true energy.

Figure 3.4 demonstrates the same behaviour more clearly, where we see the error of the approximate methods with respect to the exact value. We clearly observe a phase transition in the closed shell case, where initially HFB follows the Hartree-Fock solution perfectly, but suddenly around $g \approx 4$ the pairing effects kick in and level off the error. The levelling could be explained by noting that in the large g limit, the interaction term of the Hamiltonian starts to dominate and the ground state changes little with increasing interaction strength.

The phase transition and its relation to the pairing can be seen very clearly in figure 3.5, where we have divided up the energy into three components: kinetic and external potential, interaction, and pairing, according to

$$E = \underbrace{\mathrm{Tr}\,(T\rho)}_{\text{kin.+pot.}} + \frac{1}{2}\underbrace{\mathrm{Tr}\,(\Gamma\rho)}_{\text{interaction}} - \frac{1}{2}\underbrace{\mathrm{Tr}\,(\Delta\kappa^*)}_{\text{pairing}}$$

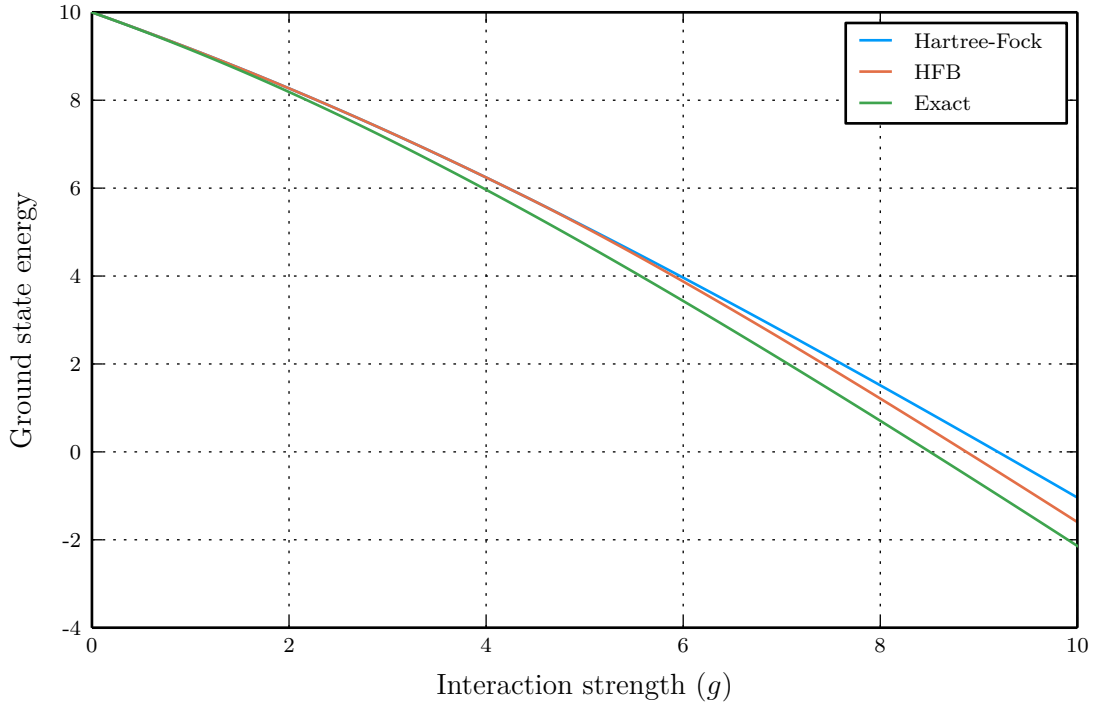

Figure 3.3: The ground state energy of a closed shell system (6 particles, 4 oscillator shells), estimated using the different methods.

We see that in the closed shell case the phase transition point is characterised by a sudden change in the behaviour of the energies, especially in the pairing energy. It does not contribute anything before the phase transition, but turns on when the interaction becomes attractive enough, also implying that after the phase transition $\kappa \neq 0$.

In the same figures (3.4, 3.5) we also see the behaviour of an open shell system, where pairing effects are always present for all interaction strengths. The relevance of pairing for the open shell system can be explained with the fact that there are multiple equivalent subshells for the particles to choose from, also seen by the degeneracy of the of the ground state in the non-interacting limit. Hence, there is no phase transition and the HFB method always has a significantly lower error when compared to the Hartree-Fock.

In general, we can see that the HFB method allows us to estimate the energy of the ground state even in the strongly attractive regime. While here we presented results for only a specific model space and few cases, the same general behaviour also holds when the number of shells or particles is changed.

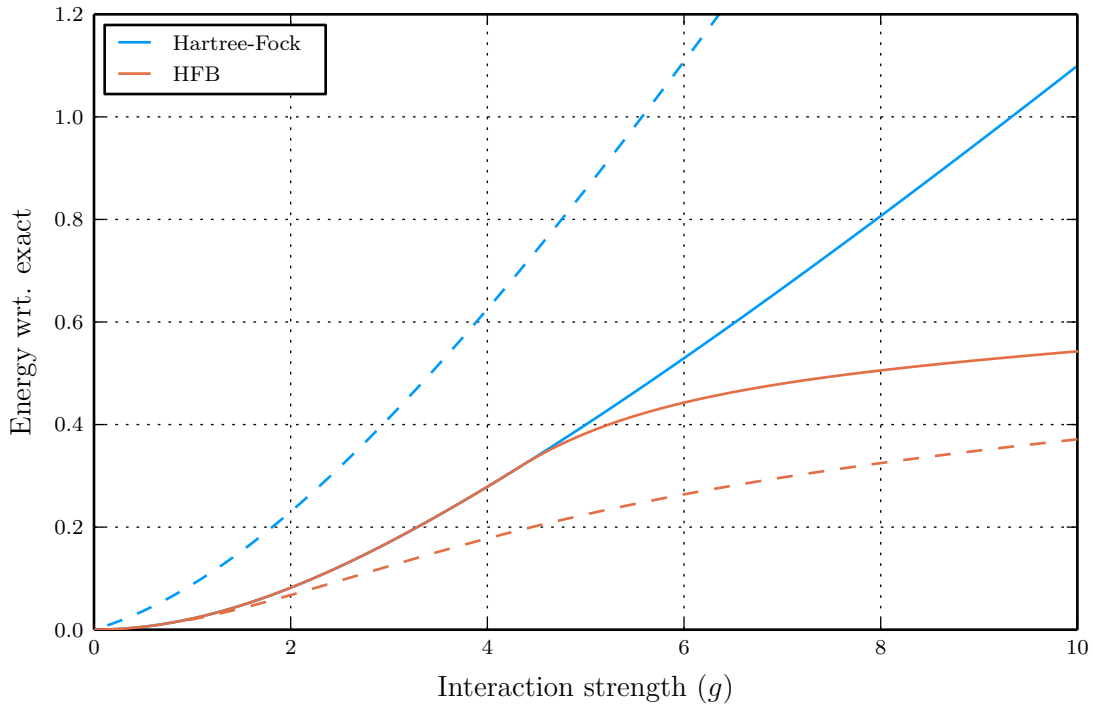

Figure 3.4: The absolute error of the HF and HFB methods with respect to the exact value. The solid lines are for a close shell (6-particle) system and dashed lines for an open shell (8-particle) system, solved in a 4-shell model space.

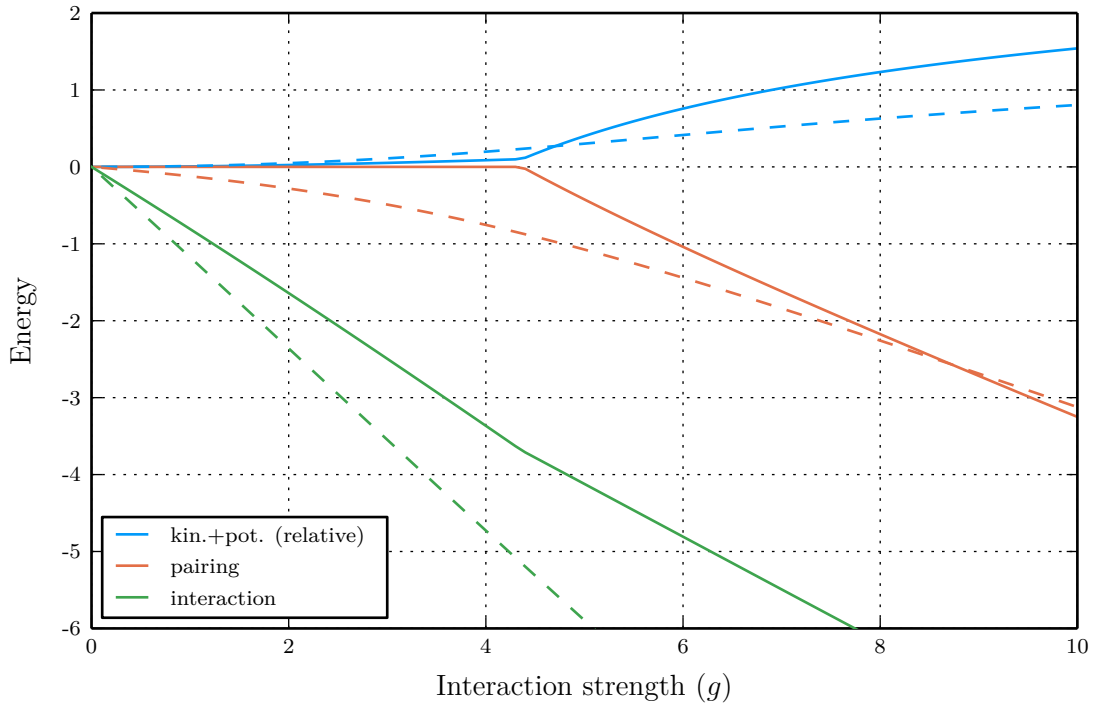

Figure 3.5: The different energy components for the same systems as on figure 3.4, with solid lines corresponding to the closed shell system and dashed lines to the open shell system. The kinetic+external potential energy is measured relative to the non-interacting value, to make it easier to interpret its variation.

Chapter 4

Quasiparticle Random Phase Approximation

With the HFB method we can calculate the ground state of the system. However, in order to get information on the excited states we turn to the quasiparticle random phase approximation (QRPA) method [18, 6, 22], which builds on top of the HFB solution[1] and approximates the system's excitations as superpositions of quasiparticle excitations.

As with the HFB, we are interested in seeing how well the QRPA method can predict the exact solutions. We will compare its predictions against the exact results and then determine whether we can use QRPA to extend the few-body, exact calculations of excitations to larger systems.

4.1 Formulation

The QRPA method can be derived from various assumptions, yielding the same equations. Here we consider an approach that is somewhat similar to how we treated the HFB, called the equations-of-motion method [21].

The starting point is a reformulation of the Schrödinger equation. Let $|-\rangle$ be the ground state of our system and $\{Q_\nu^\dagger\}$ a set of excitation operators that connect the ground state to the excited states, i.e. $|\nu\rangle = Q_\nu^\dagger |-\rangle$. Then, for every perturbation δQ the following

[1] A random phase approximation is a quite generic approach, so it can also be based upon a Hartree-Fock solution and is then referred to simply as the random phase approximation (RPA). The "quasiparticle" part in QRPA emphasises the fact that the excitations operators are built from the quasiparticle creation operators.

equation holds[2]

$$\langle -|[\delta Q, \hat{H}, Q_\nu^\dagger]|-\rangle = \hbar\omega_\nu \langle -|[\delta Q, Q_\nu^\dagger]|-\rangle$$

As long as we do not make any simplifying assumptions regarding the ground state or the excitation operators, this formulation is equivalent to the Schrödinger equation.

We can then approximate the excitation operators as superpositions of pairs of quasiparticle creation and annihilation operators as follows

$$Q_\nu^\dagger = \frac{1}{2}\sum_{ij} X_{ij}^{(\nu)}\beta_i^\dagger\beta_j^\dagger - Y_{ij}^{(\nu)}\beta_i\beta_j$$

and, analogously to the HFB, define a corresponding QRPA ground state $|\text{QRPA}\rangle$

$$\forall\nu : Q_\nu |\text{QRPA}\rangle = 0$$

With this simplification and the additional assumption that the ground state of the system is similar to the HFB ground state ($|\text{QRPA}\rangle \approx |\text{HFB}\rangle$), the QRPA equations can be derived. They can be compactly written in the following form

$$\begin{pmatrix} A & B \\ B^* & A^* \end{pmatrix}\begin{pmatrix} X^{(\nu)} \\ Y^{(\nu)} \end{pmatrix} = \hbar\omega_\nu \begin{pmatrix} X^{(\nu)} \\ -Y^{(\nu)} \end{pmatrix}$$

where $X^{(\nu)}$ and $Y^{(\nu)}$ are asymmetric matrices of the corresponding excitation operator and A and B are linear operators on those matrices. In terms of matrix elements they can be calculated as

$$\begin{aligned} A_{ijkl} &= \langle \text{HFB}|[\beta_j\beta_i, [\hat{H}, \beta_k^\dagger\beta_l^\dagger]]|\text{HFB}\rangle \\ B_{ijkl} &= -\langle \text{HFB}|[\beta_j\beta_i, [\hat{H}, \beta_k\beta_l]]|\text{HFB}\rangle \end{aligned}$$

with more explicit expression given in chapter 8 of [18].

Every solution of the QRPA equation defines an excitation operator $Q_\nu^\dagger$, which we in general assume to correspond to a physical excitation of the system. An exception are certain zero eigenvalue spurious solutions, which can arise due to broken symmetries.[3] However, the set of QRPA solutions is only a subset of all possible excitations, namely the ones that can be approximated by a superposition of two-quasiparticle excitation. This

[2]The $[A, B, C]$ is defined as the symmetric double commutator, $[A, B, C] = \frac{1}{2}\left([[A, B], C] + [A, [B, C]]\right)$.
[3]The spurious solutions to the QRPA are more thoroughly discussed in [6] and [18].

means that there is a relatively clear interpretation that every excitation either adds or removes two quasiparticles.

In terms of physical particles this means that a QRPA excitation is a superposition of excitations that either add two, remove two, or add and remove one particle. Removal of particle can be thought of as creating a "hole" in the filled state, so these excitation are referred to as particle-particle (pp), hole-hole (hh) or particle-hole (ph) excitations.

4.2 Implementation

In principle, the QRPA equation is a simple eigenvalue problem, and the most straightforward numeric implementation would be one where we construct the matrix according to the definitions and simply diagonalize it. However, due to the size of the matrix, which has a M^4 dependence on the number of the single particle orbitals (compared to the M^2 of the HFB method), this quickly becomes computationally costly as we increase the number of oscillator shells. Therefore, in this work, we opted for a scheme where the application of the QRPA operator can be calculated without constructing the whole matrix, allowing us to use iterative diagonalization routines to solve for the eigenvalues [10].

The first step in solving the QRPA for a system is calculating the ground state from the HFB, which becomes the approximation for the QRPA ground state. The HFB solution yields the matrices U and V, which represent the Bogoliubov transformation defining the ground state, and also the spectra of energies for all the quasiparticle operators, which we can organize into a diagonal matrix E, that has the energies on the diagonal.

Armed with the HFB solution, the action of the QRPA operator on the X and Y matrices defining an excitation operator can be written as

$$\text{QRPA}\begin{pmatrix} X \\ Y \end{pmatrix} = \begin{pmatrix} EX + XE + W_1(X,Y) \\ -EY - YE - W_2(X,Y) \end{pmatrix}$$

where the only complicated bits are the W_1 and W_2 matrices.

In order to make it easier to follow, the definition of W_1 and W_2 can be broken down into a number of sub-steps, that can also be implemented as separate routines in code, to make the code more readable. We first define a set of generic functions on matrices that depend on the U, V and $\bar{v}$ matrices:

$$\rho(X,Y) = UXV^T + V^*YU^\dagger, \qquad \kappa(X,Y) = UXU^T + V^*YV^\dagger$$

$$\Gamma_{ij}(\rho) = \sum_{kl} \bar{v}_{ikjl}\rho_{kl}, \qquad \Delta_{ij}(\kappa) = \frac{1}{2}\sum_{kl} \bar{v}_{ijkl}\kappa_{kl}$$

$$W(\Gamma, \Delta_1, \Delta_2) = U^\dagger \Gamma V^* + U^\dagger \Delta_1 U^* + V^\dagger \Delta_2 V^* - V^\dagger \Gamma^T U^*$$

and then we can assign them particular values, until we end up with the W_1 and W_2 as follows

$$\rho = \rho(X, Y), \quad \kappa_1 = \kappa(X, Y), \quad \kappa_2 = \kappa^\dagger(Y^\dagger, X^\dagger)$$

$$\Gamma = \Gamma(\rho), \quad \Delta_1 = \Delta(\kappa_1), \quad \Delta_2 = \Delta^\dagger(\kappa_2^\dagger)$$

$$W_1 = W(\Gamma, \Delta_1, \Delta_2), \quad W_2 = W^\dagger(\Gamma^\dagger, \Delta_2^\dagger, \Delta_1^\dagger)$$

With this operator the QRPA equation is an eigenvalue equation

$$\text{QRPA} \begin{pmatrix} X \\ Y \end{pmatrix} = \hbar\omega \begin{pmatrix} X \\ Y \end{pmatrix}$$

and, while it does not yield itself to diagonalization in this form, can be solved with iterative algorithms, specifically the Arnoldi method.

The Arnoldi method is generically implemented in ARPACK [1], and the routines available in Julia via built-in bindings. In this work we therefore simply implemented the operator according to the definitions above and passed it to the ARPACK routines. The only thing we had to keep in mind is that the X and Y matrices are antisymmetric, and therefore have only $M(M-1)/2$ independent components each. We chose the upper triangle of the matrices as the independent components and devised a simple indexing scheme to convert between the matrices and the one-dimensional vector representation used internally by ARPACK.

4.3 The excitation spectra

As a first step in studying the QRPA we look at the unmodified excitations spectra. We are interested in knowing how well it can replicate the exact spectra.

Due to the fact that the excitations are superpositions of pp-, hh- and ph-excitations, the interpretation of an excitation is non-trivial. We categorize the excitations according to the dominating component, which we determine by summing together the squares of the magnitudes of the coefficients in the expansion of the excitation operator in terms of the physical creation and annihilation operators. If a particular component is more than

half of the whole, we declare that to be the essential nature of the excitation.

Practically we can do that by calculating the sum of the matrix elements of the transition fields, i.e. $2\sum|\rho|^2$ for ph-components, $\sum|\kappa_1|^2$ for pp-components and $\sum|\kappa_2|^2$ for hh-components.

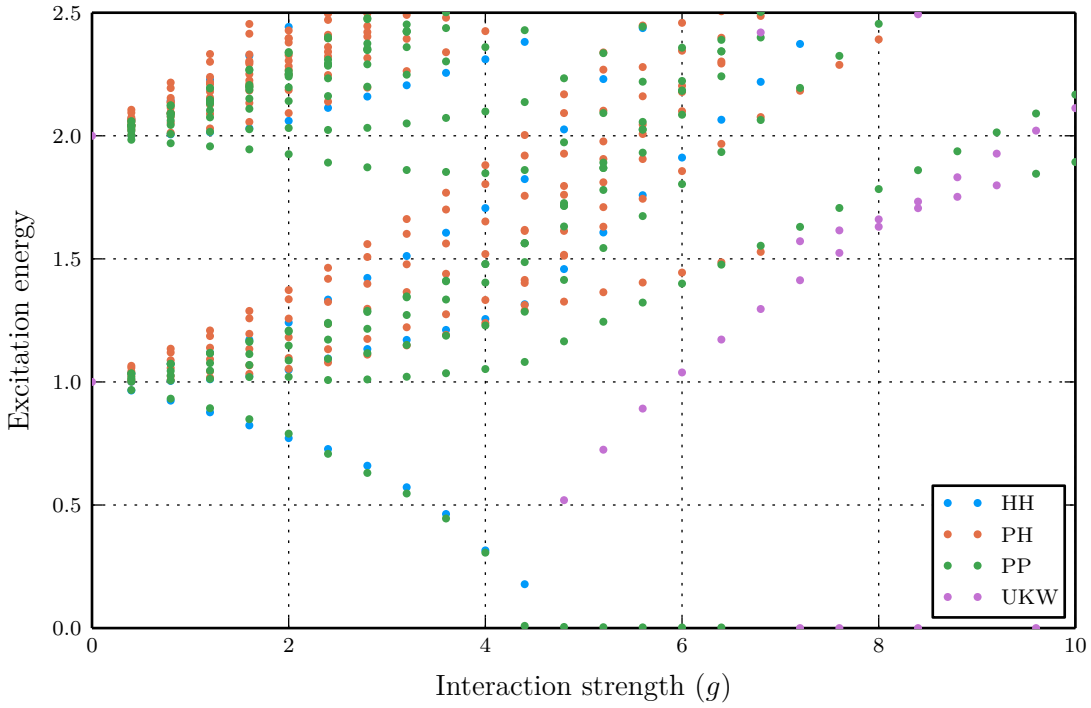

Figure 4.1: The low-lying excitations of a 6-particle closed shell system as predicted by QRPA (calculated in the 3-shell model space). The excitations are categorized according to the dominating excitation component as hole-hole (HH), particle-particle (PP), particle-hole (PH) or mixed (UKW), if no dominating component stands out.

An example of an excitation spectrum is displayed on figure 4.1, where we see the lowest excitations predicted by the QRPA for a closed-shell system. Even though the spectra are hard to interpret due to the large number of excitations, there are some things we can see clearly. First, we see that we can generally quite easily determine the types of the excitations, although it becomes harder as the interaction strength increases. In the open shell case it is usually harder to determine the type of the excitation, since the ground state will always have pairing ($\kappa \neq 0$) and then the excitations will mix systems with different particle numbers as well.

It is interesting to note that some of the excitations are clearly pp or hh, meaning

they add or remove two particles to or from the ground state. The interpretation of such excitations is that they correspond to excitations in the $A \pm 2$ particle systems.

Additionally, as one would expect, in the non-interacting limit the excitation spectra converge to degenerate sets with integer differences in energy, corresponding to the non-interacting excitations.

In the closed shell case we also see excitations that have zero energy at the phase transition. Before the phase transition point, in the normal phase, we see two states that can clearly be interpreted as states from the neighbouring systems. More precisely, since they are have the lowest energy we assume that they correspond to the ground states of the $A \pm 2$-particle systems. After the phase transition there is one mixed state, which corresponds to the Higgs mode. Also after the phase transition we always see a zero-energy excitation, which is a spurious state always present in the QRPA spectra, when the ground state break particle number symmetry due to pairing.

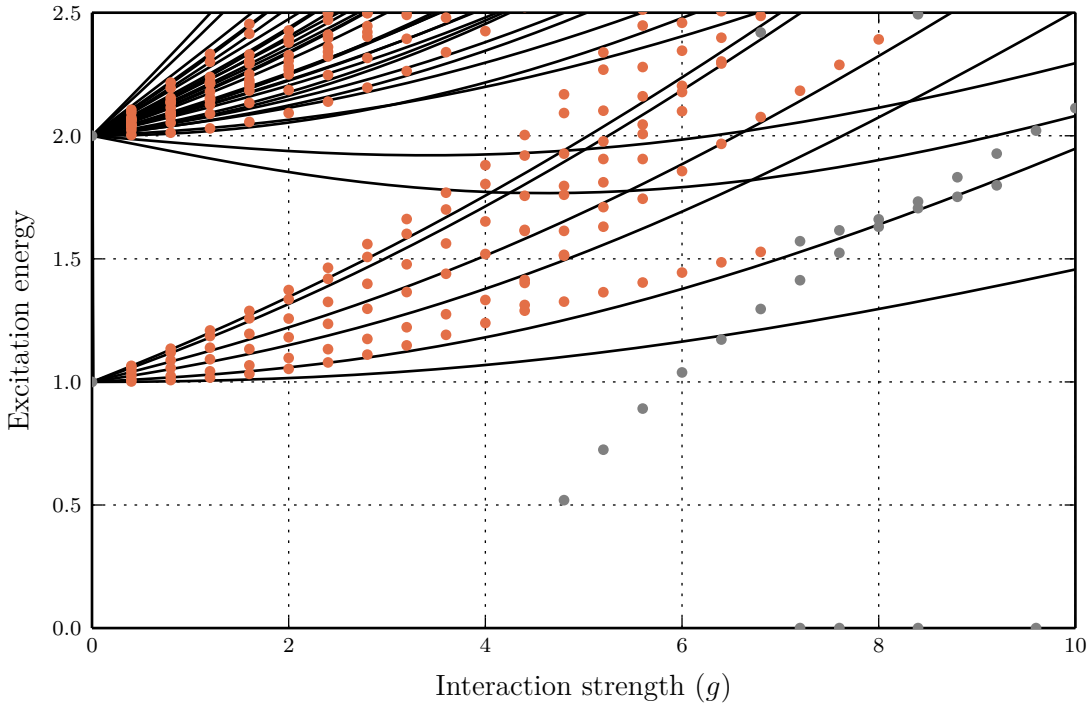

Figure 4.2: A QRPA spectrum with only ph (red) and mixed (gray) excitations of the same closed shell system as in figure 4.1, compared against the complete exact diagonalization spectrum (black lines).

Finally, figures 4.2 and 4.3 compare the QRPA spectra against the exact spectra for

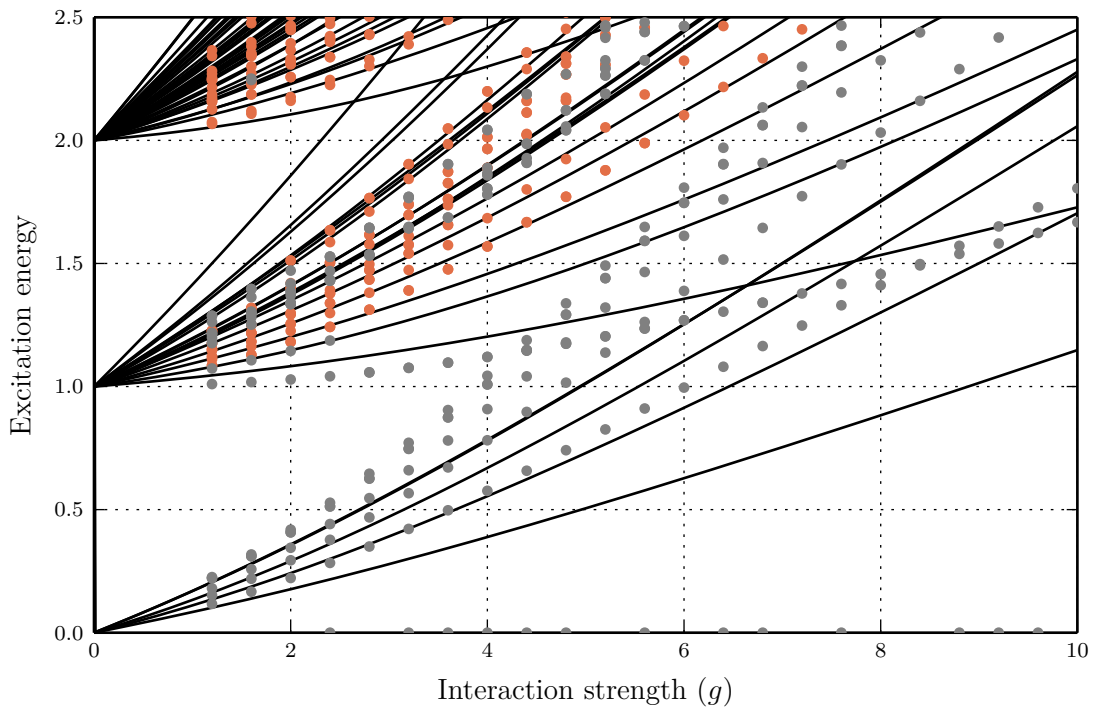

Figure 4.3: The QRPA spectrum of an open shell system (8 particles, 3 shells), compared against the complete exact diagonalization spectrum (black lines). Only the ph (red) and mixed (gray) excitations in the QRPA are shown.

closed and open shell systems, respectively. There we have only retained the clearly ph and mixed excitations, which can correspond to excitations in the same system.

In general we see that the QRPA is qualitatively able to reproduce the excitation spectra. If we count the degeneracies of the states, then we also see that the states in the QRPA spectra correspond exactly to the ones in the true spectra. This changes slightly at higher energy when 2p2h and more complicated excitations become relevant, which are expectedly not reproduced by the QRPA. An example of that are the states with a minima in figure 4.2. The energy estimates are not very accurate, however, and get worse with higher interaction strength.

4.4 Corrections to the HFB energy

A different application for the QRPA is using it to improve the HBF's estimate of the ground state energy. Using many-body perturbation theory it is possible to derive a 2nd

order correction to the ground state energy estimate [11], which relies on the matrix elements of the QRPA matrix

$$E^{(2)}_{\mathrm{MBPT}} = -\frac{1}{6} \sum_{i<j,k<l} \frac{|B_{ijkl}|^2}{E_i + E_j + E_k + E_l}$$

and a better estimate for the ground state energy is then given by $E_{\mathrm{HFB}} + E^{(2)}_{\mathrm{MBPT}}$.

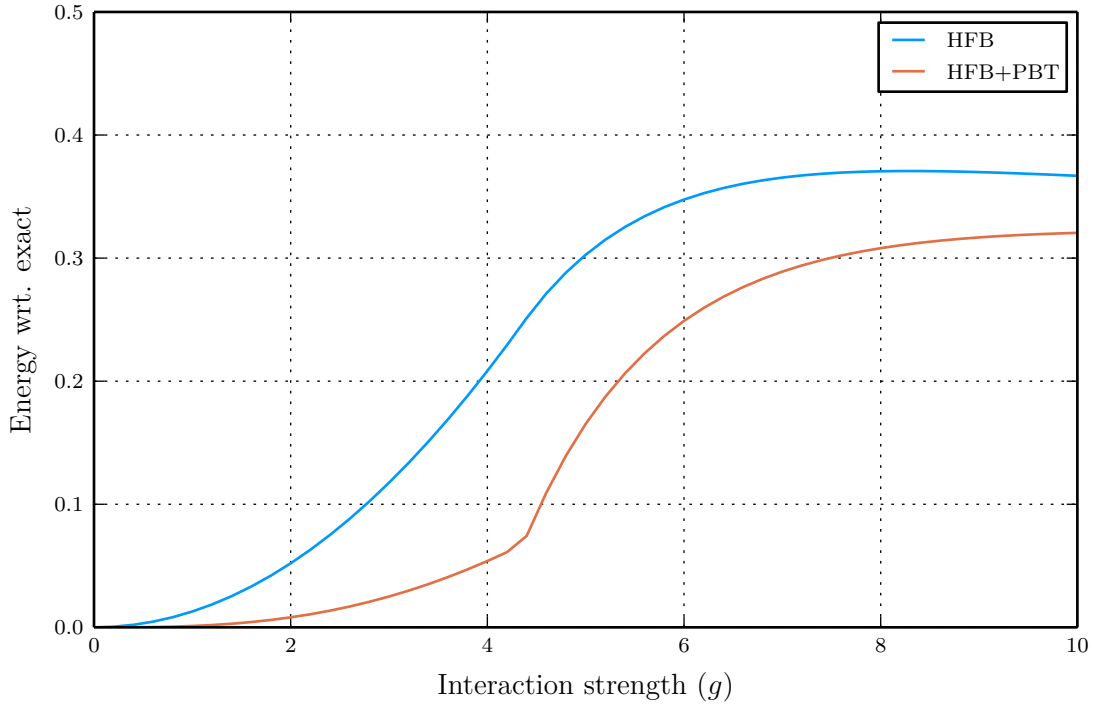

Figure 4.4: Comparison of the perturbation theory corrected and raw HFB ground state energy estimates for a closed shell (6-particle, oscillator 3-shells) system, presented with respect to the exact value.

In figure 4.4 we see the error from the exact value for the ground state energy. We see that it yields a much better result before the phase transition, but only a minor correction after the phase transition. In the open shell case, since the ground state is always paired, the correction is also always small.

4.5 Capturing the Higgs mode

As the final part of this thesis we make a preliminary attempt to calculate the lowest monopole excitation, discussed in section 2.3.1. In the non-interacting limit the excitation corresponds to a 2p2h excitation and therefore cannot be described by the QRPA excitation operator.

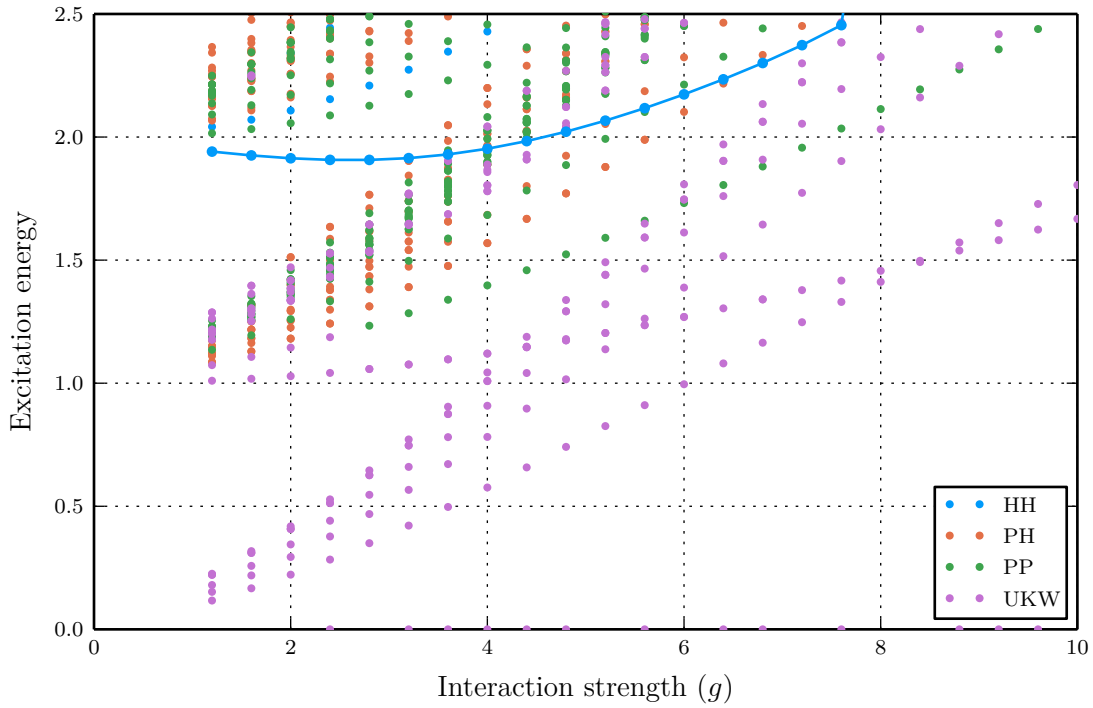

Figure 4.5: The low-lying excitations for an open shell (8 particles, 3 shells) system as predicted by QRPA. The excitations are categorized according to the dominating excitation component as hole-hole (HH), particle-particle (PP), particle-hole (PH) or mixed (UKW), if no dominating component stands out. The line emphasizes a hh-excitation with the characteristic minimum of a closed shell lowest monopole excitation.

It should, however, be possible to see this excitation in the spectra of the open shell $A \pm 2$ particle systems. For example, based on the $A - 2$ particle ground state, a pp-excitation could add particles onto the next shell, instead of filling out the shell, and therefore create an effective 2p2h hole excitation of the closed shell system. In figure 4.5 we see a hh-excitation with roughly 2 units of energy, initially going down. This is the characteristic behaviour of the energy for the lowest monopole excitation in a closed shell system, indicating that this could be the state of interest.

However, the interpretation of the excitation energy for a state from the neighbouring system is not entirely trivial. Specifically we have to keep in mind that the energies of the Bogoliubov operators are measured with respect to the chemical potential μ. Specifically the logic is following: let $\hbar\omega^{(A\pm2)}$ be the excitation energy with respect to the chemical potential in the $A \pm 2$ particle ground state. The total energy of the state can then be calculated with

$$E_\nu = \hbar\omega^{(A\pm2)} \mp 2\mu^{(A\pm2)} + E_0^{(A\pm2)}$$

By subtracting the energy of the A-particle ground state we can find the state's excitation energy in the A-particle system, which should then correspond to the exact calculations.

$$\hbar\omega_\nu^{(A)} = \hbar\omega^{(A\pm2)} \mp 2\mu^{(A\pm2)} + E_0^{(A\pm2)} - E_0^{(A)}$$

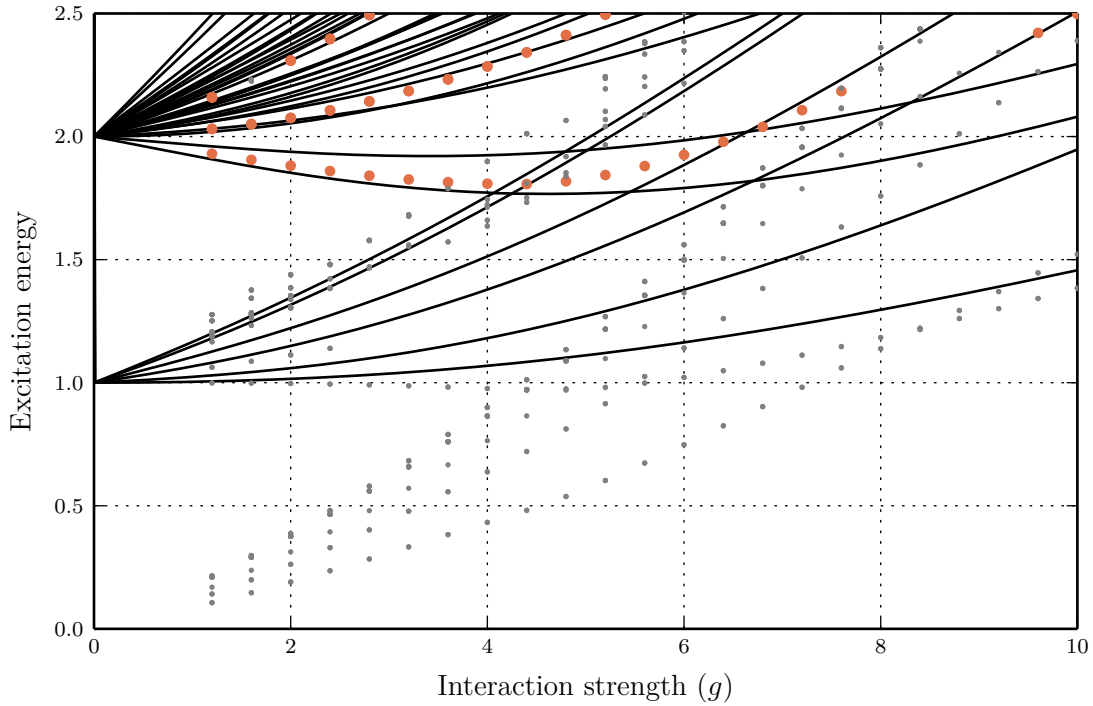

Figure 4.6: Hole-hole (red) and mixed (gray) QRPA excitations from the 8-particle system compared against the exact excitation spectrum of the 6-particle system (black lines). The QRPA energies are corrected for system shift. Both system were calculated in the 3-shell model space.

Using this formula we can correct the ground state energy and compare against exact

results. Figure 4.6 compares the excitation spectra. We see that there is agreement before the phase transition, or minima point, but the agreement worsens after the phase transition. This is likely due to the phase transition in the closed shell system, exhibiting itself in the qualitative change of the closed shell ground state energy $E_0^{(A)}$ we use to correct the excitation energy. Figure 4.7 shows the same comparison for a larger system, where we see that the QRPA also correctly predicts that the minima deepens, but the disagreement after the phase transition remains.

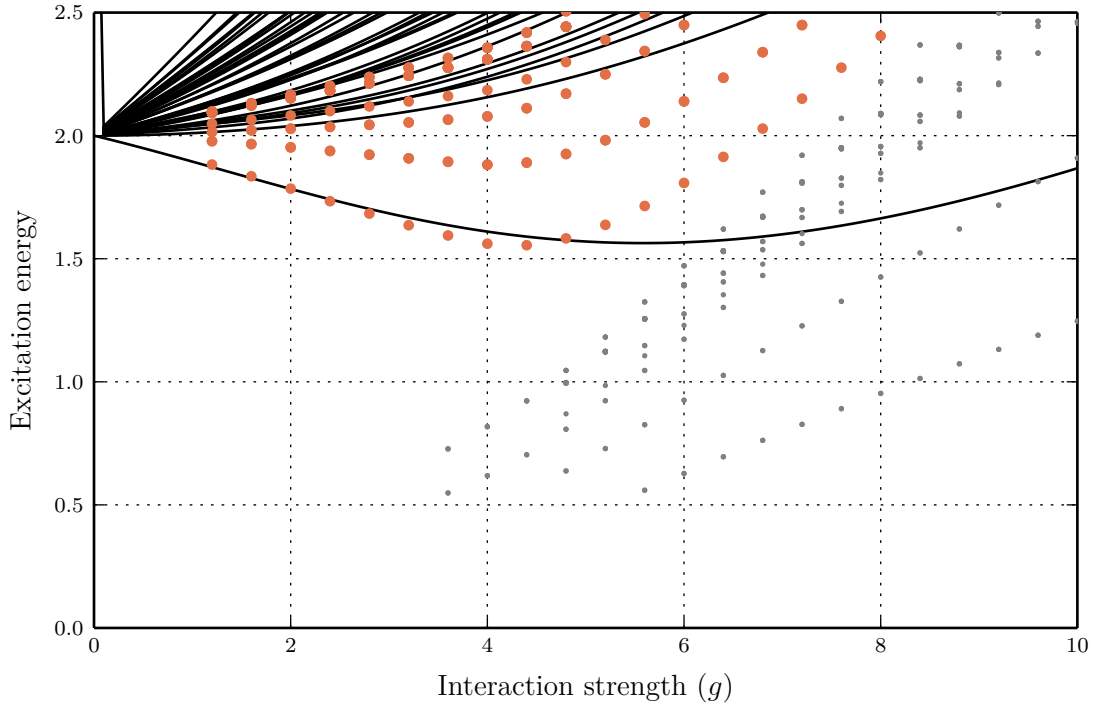

Figure 4.7: The same as figure 4.6, but for a 14-particle QRPA spectra compared to the 12-particle exact spectrum,. Both system were calculated in the 4-shell model space and the exact calculations were performed in the $L = 0$ and $S = 0$ subspace.

Chapter 5

Conclusions and outlook

In this work we applied the HFB and QRPA methods to the problem of the harmonically trapped attractively interacting Fermi gas in the few body limit. The primary purpose was to implement the methods in code and then evaluate whether the methods give reasonable results for this particular system.

We were able to show that the methods are qualitatively able to reproduce the exact results. In the ground state of a closed shell system the HFB method has a phase transition, where initially the method finds a solution that does not have any correlations, but after a certain interaction strength, pairing effects take hold. In the open shell case the pairing is always present due to the degeneracy of the ground state in the non-interacting limit.

The HFB method allows us to estimate the ground state energy, which remains in good agreement with the exact energy even as the interaction strength increases. The QRPA method allows us to improve the agreement even more, especially in the normal phase.

Additionally, we were able to see that the QRPA method qualitatively replicates the excitation spectra, even though the agreement in energy is not ideal, especially in the superfluid phase. We also showed that in principle it is possible to get access to two-particle-two-hole excitations by computing the spectra of the ± 2 particle systems and then appropriately correcting the energy.

Outlook. The driving motivator of this work was the wish to replicate the Higgs-mode excitations using these mean-field methods. We were able to achieve a very preliminary result, although more work is necessary, especially in order to verify that the results in this work also converge as they do in the exact method as the basis size is increased.

Alternatively, to capture the Higgs mode, we could employ a HFB scheme where we

try to minimize the HFB to an excited state. By wisely choosing the HFB excitation we could reach the monopole excitation. The QRPA could then be used to correct the energy of that state as well.

In addition to that, there are other methods that can be constructed on top of these that could be used to extend this work. As an example, the Lipkin-Nogami method [25] could be used to improve the ground state estimate of the HFB. The QRPA spectra would also be improved if the Lipkin-Nogami state is used instead of the ordinary HFB state as the approximation for the QRPA ground state.

All in all, the approach studied in this work shows promise in calculating the ground and excited states in the few-body limit. It could then function as a tool for exploring the few-body limit but for larger and more complex systems.

Bibliography

[1] The ARPACK software. `http://www.caam.rice.edu/software/ARPACK/`.

[2] The Julia Language. `http://julialang.org/`.

[3] M. Bender, P.-H. Heenen, and P.-G. Reinhard. Self-consistent mean-field models for nuclear structure. *Reviews of Modern Physics*, 75(1):121, 2003.

[4] J. Bezanson, A. Edelman, S. Karpinski, and V. B. Shah. Julia: A fresh approach to numerical computing. *arXiv preprint arXiv:1411.1607*, 2014.

[5] J. Bjerlin, S. M. Reimann, and G. M. Bruun. Few-body precursor of the higgs mode in a fermi gas. *Physical Review Letters*, 116(15):155302, 2016.

[6] J. Blaizot and G. Ripka. *Quantum Theory of Finite Systems*. Cambridge, MA, 1986.

[7] I. Bloch, J. Dalibard, and S. Nascimbène. Quantum simulations with ultracold quantum gases. *Nature Physics*, 8(4):267–276, 2012.

[8] I. Bloch, J. Dalibard, and W. Zwerger. Many-body physics with ultracold gases. *Reviews of Modern Physics*, 80:885–964, 2008.

[9] G. M. Bruun. Long-lived higgs mode in a two-dimensional confined fermi system. *Physical Review A*, 90(2):023621, 2014.

[10] B. G. Carlsson, J. Toivanen, and A. Pastore. Collective vibrational states within the fast iterative quasiparticle random-phase approximation method. *Physical Review C*, 86(1):014307, 2012.

[11] B. G. Carlsson, J. Toivanen, and U. von Barth. Fluctuating parts of nuclear ground-state correlation energies. *Physical Review C*, 87(5):054303, 2013.

[12] C. Chin, R. Grimm, P. Julienne, and E. Tiesinga. Feshbach resonances in ultracold gases. *Reviews of Modern Physics*, 82:1225–1286, 2010.

[13] J. Christensson Cremon. *Quantum Few-Body Physics with the Configuration Interaction Approach: Method Development and Application to Physical Systems*. PhD thesis, Lund University, 2010.

[14] C. J. Cramer et al. Essential of computational chemistry. *Wiley, England*, 2004.

[15] F. Deuretzbacher. *Spinor Tonks-Girardeau gases and ultracold molecules*. PhD thesis, University of Hamburg, 2008.

[16] A. Fetter and J. Walecka. *Quantum Theory of Many-particle Systems*. Dover Books on Physics. Dover Publications, 2003.

[17] P. Navrátil, S. Quaglioni, I. Stetcu, and B. R. Barrett. Recent developments in no-core shell-model calculations. *Journal of Physics G: Nuclear and Particle Physics*, 36(8):083101, 2009.

[18] P. Ring and P. Schuck. *The Nuclear Many-Body Problem*. Physics and astronomy online library. Springer, 2004.

[19] S. Roman. *Advanced Linear Algebra*, volume 3. Springer, 2005.

[20] M. Rontani, S. Åberg, and S. Reimann. Configuration interaction approach to the few-body problem in a two-dimensional harmonic trap with contact interaction. *arXiv preprint arXiv:0810.4305*, 2008.

[21] D. Rowe. Equations-of-motion method and the extended shell model. *Reviews of Modern Physics*, 40(1):153, 1968.

[22] D. J. Rowe. *Nuclear collective motion: models and theory*. World Scientific, 2010.

[23] J. J. Sakurai and J. Napolitano. *Modern quantum mechanics; 2nd ed.* Addison-Wesley, San Francisco, CA, 2011.

[24] F. Serwane, G. Zürn, T. Lompe, T. Ottenstein, A. Wenz, and S. Jochim. Deterministic preparation of a tunable few-fermion system. *Science*, 332(6027):336–338, 2011.

[25] J. Suhonen. *From Nucleons to Nucleus: Concepts of Microscopic Nuclear Theory*. Springer Science & Business Media, 2007.

[26] A. Wenz, G. Zürn, S. Murmann, I. Brouzos, T. Lompe, and S. Jochim. From few to many: observing the formation of a fermi sea one atom at a time. *Science*, 342(6157):457–460, 2013.

[27] G. Zürn, A. N. Wenz, S. Murmann, A. Bergschneider, T. Lompe, and S. Jochim. Pairing in few-fermion systems with attractive interactions. *Physical Review Letters*, 111:175302, 2013.

Acknowledgements

First and foremost, I want to thank my supervisors, Stephanie Reimann and Gillis Carlsson, for their time, guidance, feedback and support, and for providing an engaging topic to work on. I learned much from this project, both about physics and the life in the academia, and both the work and long discussions were great fun.

Similarly, I wish to thank Johannes Bjerlin and Georg Bruun, for the many hours of enlightening discussions, giving good insights. I would also like to recognize all the people at Mathematical Physics, for providing a homely environment, good company and all the cake and coffee that fuelled this work.

Finally, I would like to acknowledge the financial support of the Archimedes Foundation and the Estonian Ministry of Education and Research, under the Kristjan Jaak scholarship.

Appendix A

Harmonic oscillator in 2D

We work exclusively in the harmonic oscillator basis, meaning that we always construct our basis from the one-dimensional harmonic oscillator basis.

In one dimension the harmonic oscillator Hamiltonian is

$$\hat{H} = \frac{\hat{p}^2}{2m} + \frac{m\omega^2}{2}\hat{x}^2 = \hbar\omega\left(\hat{N} + \frac{1}{2}\right)$$

and the following set of functions for $n = 0, 1, \ldots$ form a complete eigenbasis with eigenvalues $E_n = \hbar\omega\left(n + \frac{1}{2}\right)$

$$\Psi_n(\tilde{x}) = \frac{1}{\pi^{1/4}\sqrt{x_0 2^n n!}} H_n(\tilde{x}) \exp(-\tilde{x}^2/2)$$

where $\tilde{x} = x/x_0 = x\sqrt{m\omega/\hbar}$ and $H_n(\tilde{x})$ are the physicist's Hermite polynomials characterized by the recursion relation

$$H_0(\tilde{x}) = 1, \quad H_{n+1}(\tilde{x}) = 2\tilde{x}H_n(\tilde{x}) - H_n'(\tilde{x})$$

The two-dimensional basis for fermions can then be constructed by taking the tensor product of two of these and a two-dimensional Hilbert space to account for spin. We can then label all the basis states as $|m, n, s\rangle$, where $m, n \in \{0, 1, \ldots\}$ and $s \in \{\uparrow, \downarrow\}$, and the wave function over $x, y \in \mathbb{R}$ and $s \in \{\uparrow, \downarrow\}$ is then given as

$$\psi_{m,n,s_0}(x, y, s) = \Psi_m(x/x_0)\Psi_n(y/y_0)\delta_{s,s_0}$$

Since we have to deal with multiple particles, it is convenient merge the different coordinates

into a single identifier, i.e. $q = (x, y, s)$. Integration over q is then understood to be separate integrations over all the continuous variables and summation over the discrete ones, i.e. $\int \mathrm{d}q = \sum_s \int\int \mathrm{d}x\, \mathrm{d}y$.

These states are the eigenstates of the hamiltonian of the two-dimensional harmonic oscillator

$$\hat{H} = \hbar\omega \left(\hat{N}_x + \hat{N}_y + 1\right)$$

and so this Hamiltonian is diagonal in this basis, i.e.

$$\langle m, n, s|\hat{H}|m', n', s'\rangle = \hbar\omega \left(m + n + 1\right) \delta_{m,m'}\delta_{n,n'}\delta_{s,s'}$$

In the implementation we need to have a correspondence between a single linear index i and the identifiers of the basis states $i \leftrightarrow (m_i, n_i, s_i)$, which we implemented as a simple lookup table. It should just be noted that it is convenient if the mapping does not depend on the truncation of the single particle basis, meaning that the correspondence of the lower shells is not changed if shells are added to the system. So, it should go as $0 \to (0, 0, \uparrow)$, $1 \to (0, 0, \downarrow)$, $2 \to (1, 0, \uparrow)$, $3 \to (1, 0, \downarrow)$, $4 \to (0, 1, \uparrow)$, $5 \to (0, 1, \downarrow)$, ..., so that 0 and 1 always refer to the first shell, 2-5 to the second shell and so on.

Contact interaction. The interaction used in this work is the contact interaction, which is described in the wave function representation by the delta function in space. We can then calculate the matrix elements as

$$\begin{aligned}\langle ij|\hat{V}|kl\rangle &= -g \int \mathrm{d}q_1\, \mathrm{d}q_2\ \psi_i^*(q_1)\psi_j^*(q_2)\delta(x_1 - x_2)\delta(y_1 - y_2)\psi_k(q_1)\psi_l(q_2) \\ &= -g \cdot x_0 W(m_i, m_j, m_k, m_l) \cdot y_0 W(n_i, n_j, n_k, n_l) \cdot \delta(s_i, s_k) \cdot \delta(s_j, s_l)\end{aligned}$$

where we have been able to break the integration into a product of simpler expressions. The $\delta(i, j) = \delta_{ij}$ and W is given as a one-dimensional integral

$$W(i, j, k, l) = \int \mathrm{d}\tilde{x}\ \Psi_i^*(\tilde{x})\Psi_j^*(\tilde{x})\Psi_k(\tilde{x})\Psi_l(\tilde{x})$$

In this work we opted to calculate the integrals of the W using numeric integration. However, a recursion relation can also be derived, which can make the construction of the matrix significantly faster [15].